New Phytologist

FIGL1 attenuates meiotic interhomolog repair and is counteracted by the RAD51 paralog XRCC2 and the chromosome axis protein ASY1 during meiosis

Côme Emmenecker[1,2], Simine Pakzad[1], Fatou Ture[1], Julie Guerin[1], Aurélie Hurel[1], Aurélie Chambon[1], Chloé Girard[3], Raphael Mercier[4] and Rajeev Kumar[1]

[1]Université Paris-Saclay, INRAE, AgroParisTech, Institut Jean-Pierre Bourgin for Plant Sciences (IJPB), 78000, Versailles, France; [2]University of Paris-Sud, Université Paris-Saclay, 91405, Orsay, France; [3]Meiotic Recombination and Pairing Team, Université Paris-Saclay, Commissariat à l'Énergie Atomiques et aux Énergies Alternatives (CEA), Centre National de la Recherche Scientifique (CNRS), Institute for Integrative Biology of the Cell (I2BC), 91190, Gif-sur-Yvette, France; [4]Department of Chromosome Biology, Max Planck Institute for Plant Breeding Research, Carl-von-Linné-Weg 10, Cologne, Germany

Author for correspondence:
Rajeev Kumar
Email: rajeev.kumar@inrae.fr

Received: *7 May 2024*
Accepted: *16 September 2024*

New Phytologist (2024) **244:** 2442–2457
doi: 10.1111/nph.20181

Key words: chromosome axis, crossovers, DMC1, FIGL1, meiotic DNA repair, RAD51.

Summary

- Two recombinases, RAD51 and DMC1, catalyze meiotic break repair to ensure crossovers (COs) between homologous chromosomes (interhomolog) rather than between sisters (intersister). FIDGETIN-LIKE-1 (FIGL1) downregulates both recombinases. However, the understanding of how FIGL1 functions in meiotic repair remains limited. Here, we discover new genetic interactions of *Arabidopsis thaliana FIGL1* that are important *in vivo* determinants of meiotic repair outcome.
- In *figl1* mutants, compromising RAD51-dependent repair, either through the loss of RAD51 paralogs (RAD51B or XRCC2) or RAD54 or by inhibiting RAD51 catalytic activity, results in either unrepaired breaks or meiotic CO defects. Further, XRCC2 physically interacts with FIGL1 and partially counteracts FIGL1 activity for RAD51 focus formation. Our data indicate that RAD51-mediated repair mechanisms compensate FIGL1 dysfunction.
- FIGL1 is not necessary for intersister repair in *dmc1* but is essential for the completion of meiotic repair in mutants such as *asy1* that have impaired DMC1 functions and interhomolog bias. We show that FIGL1 attenuates interhomolog repair, and ASY1 counteracts FIGL1 to promote interhomolog recombination.
- Altogether, this study underlines that multiple factors can counteract FIGL1 activity to promote accurate meiotic repair.

Introduction

During meiosis, the repair of DNA double-stranded breaks (DSBs) by homologous recombination (HR) yields crossovers (COs) and noncrossovers (NCOs) (Hunter, 2015; Wang & Copenhaver, 2018). Meiotic COs between homologous chromosomes (interhomolog) rather than between sister chromatids (intersister) serve important mechanical and evolutionary roles (Schwacha & Kleckner, 1994, 1997). The choice of the sister or nonsister chromatid template for repair is thus a key determinant for the outcome of meiotic recombination.

DNA strand exchange recombinases are central in regulating the choice of DNA template for DSB repair (Brown & Bishop, 2014; Humphryes & Hochwagen, 2014). RAD51 and DMC1 recombinases are two eukaryotic RecA homologs and can assemble into nucleofilaments on single-stranded DNA (ssDNA) generated from the processing of DSBs (Sheridan *et al.*, 2008; Brown & Bishop, 2014). Both recombinases can perform homology searches of the genome and strand invasion on the donor template during meiosis. Cytologically, RAD51 and DMC1 form nuclear foci on meiotic chromosomes (Bishop, 1994; Kurzbauer *et al.*, 2012; Brown *et al.*, 2015; Slotman *et al.*, 2020). Studies in many species contend that meiotic break repair occurs in two temporally distinct phases: a DMC1-permissive phase (Phase 1) followed by a RAD51-permissive phase (Phase 2) (Hayashi *et al.*, 2007; Kim *et al.*, 2010; Crismani *et al.*, 2013; Enguita-Marruedo *et al.*, 2019; Toraason *et al.*, 2021; Ziesel *et al.*, 2022). In the DMC1-permissive phase, DMC1 predominantly repairs DSBs and catalyzes interhomolog recombination, whereas RAD51 is kept catalytically inactive (Tsubouchi & Roeder, 2006; Busygina *et al.*, 2008; Niu *et al.*, 2009; Lao *et al.*, 2013; Callender *et al.*, 2016). In the RAD51-permissive phase, the RAD51-mediated pathway becomes active to repair remaining DSBs, mainly using sister chromatids (Crismani *et al.*, 2013; Enguita-Marruedo *et al.*, 2019; Toraason *et al.*, 2021; Ziesel

et al., 2022). The RAD51-dependent pathway also repairs DSB on sisters before meiotic entry (Joshi *et al.*, 2015).

During Phase 1, different RAD51-inhibiting strategies appear to have evolved in eukaryotic species. The Mek1-mediated pathway downregulates Rad51-dependent repair in budding yeast (Niu *et al.*, 2009; Callender *et al.*, 2016). This regulation is, however, not conserved in plants, because RAD51 can repair breaks in the absence of DMC1, albeit using sister chromatids inferred from a lack of interhomolog COs (Couteau *et al.*, 1999; Wang *et al.*, 2016). The mere presence of DMC1 attenuates RAD51 repair in yeast and Arabidopsis (Lao *et al.*, 2013; Da Ines *et al.*, 2022). Constitutive activation of Rad51, in addition to active Dmc1, elicits a longer repair time in yeast (Ziesel *et al.*, 2022). Wild-type (WT) DMC1-mediated interhomolog recombination nonetheless requires the presence of RAD51, but not its catalytic activity (Cloud *et al.*, 2012; Da Ines *et al.*, 2013b). In Arabidopsis, RAD51 fused to GFP at its C-terminus (RAD51-GFP) is catalytically inactive and unable to repair breaks in mitotic and meiotic cells but supports DMC1-mediated repair during meiosis (Da Ines *et al.*, 2013b). This function suggests that the catalytic activity of RAD51 is nonessential for DMC1-mediated repair in plants.

In vivo functions of DMC1 and RAD51 require many accessory proteins in eukaryotes. In plants, BRCA2 mediates the formation of RAD51 and DMC1 foci, whereas SDS is specifically required for DMC1 focus formation (Azumi, 2002; Seeliger *et al.*, 2012; Fu *et al.*, 2020). These mediators appear to act *in vivo* at the nucleofilament formation step. Further, MND1 and HOP2 are two evolutionarily conserved proteins required for the DNA exchange activity of DMC1 in plants (Petukhova *et al.*, 2005; Chan *et al.*, 2014; Uanschou *et al.*, 2014). In *mnd1* and *hop2*, DMC1 hyperaccumulation inhibits meiotic DSB repair in Arabidopsis (Kerzendorfer *et al.*, 2006; Panoli *et al.*, 2006; Vignard *et al.*, 2007; Stronghill *et al.*, 2010; Farahani-Tafreshi *et al.*, 2022). However, weak DMC1 activity in the Arabidopsis *hop2-2* hypomorphic mutant greatly compromises interhomolog repair and allows RAD51-dependent DSB repair on sisters (Uanschou *et al.*, 2014). RAD54 is also required for RAD51 functions but is unnecessary for meiotic DSB repair in the presence of DMC1 in Arabidopsis (Hernandez Sanchez-Rebato *et al.*, 2021). Further, Arabidopsis has five structurally related RAD51 paralogs: RAD51C, XRCC3, RAD51D, RAD51B, and XRCC2 (Bleuyard *et al.*, 2005). These paralogs can form a tetrameric complex called the BCDX2 complex (Osakabe *et al.*, 2002). Arabidopsis RAD51C and XRCC3 are essential for RAD51 focus formation and meiotic repair (Bleuyard & White, 2004; Abe *et al.*, 2005; Vignard *et al.*, 2007), but RAD51B, RAD51D, and XRCC2 play no critical role in RAD51-dependent meiotic DSB repair, irrespective of the presence or absence of DMC1 (Bleuyard *et al.*, 2005; Hernandez Sanchez-Rebato *et al.*, 2021). However, the loss of Arabidopsis RAD51B and XRCC2 slightly increases the meiotic recombination rate, implying their as yet unascertained roles in meiotic repair (Da Ines *et al.*, 2013a).

Meiotic chromosome axis proteins ensure DSB repair and CO formation between homologs in a process called interhomolog bias (Morgan *et al.*, 2023). Arabidopsis ASY1, ASY3, and ASY4 are three meiotic axis-associated proteins that promote synapsis, a process allowing tethering between homologs through polymerization of synaptonemal complex (SC) proteins such as ZYP1 (Caryl *et al.*, 2000; Armstrong *et al.*, 2002; Higgins *et al.*, 2005; Sanchez-Moran *et al.*, 2007; Ferdous *et al.*, 2012; Chambon *et al.*, 2018; Vrielynck *et al.*, 2023). ASY1 localizes on the meiotic axis in an ASY3-dependent manner and is depleted from synapsed regions, following SC assembly between homologs (Ferdous *et al.*, 2012). Loss of ASY1, ASY3, and ASY4 results in a substantial reduction in interhomolog COs, albeit at different magnitudes, with meiotic DSBs predominantly repaired on sisters. ASY1 is required for DMC1 stabilization, suggesting a functional relationship between the meiotic axis and repair machinery (Sanchez-Moran *et al.*, 2007). How meiotic chromosome axis proteins promote DSB repair between homologs is currently unclear.

Most eukaryotes have two classes of COs formed between homologs. In Arabidopsis, class I constitutes a significant proportion (85–90%) of COs, mediated by the ZMM group of proteins (SHOC1, PTD, HEI10, ZIP4, MSH4/5, and MER3) and MLH1/3 (Mercier *et al.*, 2015). The class I CO pathway ensures the obligate CO between homologs but is sensitive to CO inference that avoids the formation of additional class I COs in close proximity (Wang *et al.*, 2015; Lloyd, 2023). Class II COs are derived from the structure-specific endonuclease-dependent pathway, including MUS81 (Berchowitz *et al.*, 2007; Wang & Copenhaver, 2018). Three nonredundant anti-class II CO pathways involving FANCM, RECQ4A & RECQ4B, and FIDGETIN-LIKE-1 (FIGL1) limit meiotic COs through distinct mechanisms (Crismani *et al.*, 2012; Girard *et al.*, 2014, 2015; Séguéla-Arnaud *et al.*, 2015, 2017; Fernandes *et al.*, 2018a). Although these three pathways regulate class II COs, FIGL1 can also control the distribution of class I COs among chromosomes (Fernandes *et al.*, 2018a; Li *et al.*, 2021). Arabidopsis mutants lacking FIGL1 show a moderate increase in COs with occasional achiasmatic chromosomes (Girard *et al.*, 2015; Fernandes *et al.*, 2018a).

FIGL1 is a member of the AAA-ATPase family and has enigmatic roles in positively and negatively regulating meiotic CO formation. Arabidopsis and wheat FIGL1 limit class II COs potentially by preventing aberrant recombination intermediates or chromosome associations (Girard *et al.*, 2015; Fernandes *et al.*, 2018a; Kumar *et al.*, 2019; Osman *et al.*, 2024). FIGL1 and its mammalian ortholog FIGNL1 physically interact with the two recombinases and can antagonize positive mediators of RAD51/DMC1, such as BRCA2 and SDS in Arabidopsis or SWSAP1 in humans (Girard *et al.*, 2015; Fernandes *et al.*, 2018a; Kumar *et al.*, 2019; Matsuzaki *et al.*, 2019). Surprisingly, maize FIGL1 can act cooperatively with BRCA2 to positively regulate meiotic recombination (T. Zhang *et al.*, 2023). *Arabidopsis figl1*, rice *figl1*, and mice *fignl1*^{cko} mutants show a change in the dynamics of RAD51 and DMC1 foci, leading to the deregulation of strand invasion, which supports a conserved role of FIGL1/FIGNL1 in meiotic DSB repair (Zhang *et al.*, 2017; Fernandes *et al.*, 2018a; Yang *et al.*, 2022; Ito *et al.*, 2023; Q. Zhang

et al., 2023). FIGNL1 is also involved in DSB repair via homologous recombination in somatic cells (Yuan & Chen, 2013; Matsuzaki *et al.*, 2019). FIGL1/FIGNL1 is thus a conserved regulator of RAD51- and DMC1-mediated strand invasion and may function in the fine-tuned regulation of the strand invasion step to promote accurate meiotic DSB repair. How FIGL1 regulates the outcome of meiotic break repair when RAD51- and/or DMC1-dependent pathways are fully or partially impaired remains unknown. In this study, we investigated the impact of the functional relationship of *FIGL1* with components of HR repair machinery and chromosome axis genes on the outcome of meiotic DSB repair. We demonstrate that these genetic interactions are an essential determinant of meiotic break repair outcomes.

Materials and Methods

Plant growth and genetic material

Arabidopsis (*Arabidopsis thaliana*) plants were cultivated in the glasshouse or growth chamber with 16 h: 8 h, light : dark photoperiod at 20°C. Arabidopsis accession Columbia (Col.0) was the WT reference. The following Arabidopsis lines were used in this study: *figl1* (figl1-1) (Girard *et al.*, 2015), *rad51* (GABI_134A01), *RAD51-GFP* (Da Ines *et al.*, 2013b), *mnd1* (SALK_110052), *dmc1* (SAIL_170_F08), *rad51b* (SALK_024755), *xrcc2* (SALK_029106), *asy1* (SALK_046272), *asy3* (SALK_143676), *asy4* (SK22114, CS1006148) (Chambon *et al.*, 2018), and *rad54-2* (SALK_124992) (Hernandez Sanchez-Rebato *et al.*, 2021). Only the *hop2-2* allele (EYU48) (Uanschou *et al.*, 2014) was used in a Wassilewskija (Ws) ecotype background. Haploid *figl1* plants were produced by crossing Genome Elimination (GEM) lines (Ravi & Chan, 2010) with $figl1^{+/-}$ heterozygous plants.

Fertility analysis

Fertility of plants was examined by counting seeds per silique (fruit) on the scanned image of siliques fixed in 70% ethanol using the Zeiss ZEN software. At least 10 siliques per plant were sampled, and sister WT plants in the segregating population cultivated together with the mutants were used as controls. The unpaired Kruskal–Wallis test corrected by Dunn's test for multiple comparisons was used to compare the average number of seeds per silique (using the PRISM 9.3.1, GraphPad Software, Boston, MA, USA).

Cytological techniques

The surface spreads of meiotic chromosomes from pollen mother cells were prepared as previously described (Ross *et al.*, 1996). Chromosomes were visualized by staining with DAPI (1 μg ml^{-1}). The immunolocalization of MLH1 and HEI10 was performed on male meiocytes with a technique that preserves the 3D structure of the meiocyte nucleus, as described previously (Hurel *et al.*, 2018). For cytological detection of RAD51, DMC1, and REC8, male meiotic chromosome spreads from prophase I were prepared as described previously (Armstrong *et al.*, 2002). Slides of spreads were either immediately used for immunocytology or stored at −80°C before immunostaining. Chromosome axis protein REC8 and SC protein ZYP1 staining were performed to identify prophase I cells. The primary antibodies used were as follows: rabbit or rat α-REC8 (1 : 250) (Cromer *et al.*, 2013), rat α-RAD51 (1 : 500) (Kurzbauer *et al.*, 2012), rabbit α-DMC1 (1 : 200) (Da Ines *et al.*, 2022), guinea pig α-ZYP1 (1 : 250), rabbit α-MLH1 (1 : 1000) (Chelysheva *et al.*, 2010), chicken α-HEI10 (1 : 10000) (Chelysheva *et al.*, 2012), and rat α-ZYP (Higgins *et al.*, 2005). Secondary antibodies used were conjugated with Alexa Fluor 488 (A27034; Thermo Fisher Scientific, Waltham, MA, USA), Alexa Fluor 568 (A11041; Thermo Fisher Scientific), and Alexa Fluor 647 (A21247; Thermo Fisher Scientific).

For the chromosome spreads and 3D immunolocalization, images were acquired using the ZEISS Axio Imager 2 microscope with a ×100 oil immersion objective driven by ZEN 2 Software (Carl Zeiss Microscopy). MLH1-HEI10 cofoci counts were performed using the IMARIS software (Oxford Instruments, Oxfordshire, UK), and chromosome spreads were analyzed using the ZEN software. RAD51 and DMC1 foci were counted using FIJI as described previously (Fernandes *et al.*, 2018a). The unpaired Kruskal–Wallis test corrected by Dunn's test for multiple comparisons was used for the comparison of (1) the average number of MLH1-HEI10 cofoci per cell, (2) the average number of bivalents per cell, and (3) the mean number of RAD51 and DMC1 foci per cell using the PRISM GRAPHPAD 9.3.1 software.

AlphaFold2 predictions

AlphaFold2 predictions for protein complexes between XRCC2 and FRBD-FIGL1 were computed through the ColabFold notebook (ColabFold v.1.5.5 and AlphaFold2 v.2.2) using a Colab-Pro+ plan (https://colab.research.google.com/github/sokrypton/ColabFold/blob/main/AlphaFold2.ipynb). The plDDT, PAE, and ipTM scores and graphs were provided directly by this notebook. No template information was used for structure prediction. The predicted structures were not relaxed using amber. mmseqs_uniref_env was used for the unpaired MSA, and sequences from the same species were paired. For the advanced settings, the automatic modes were applied, only one seed was used, and dropouts were not enabled. The UCSF CHIMERAX (v.1.7.1) was used for producing images in figure.

Yeast two-hybrid assays

The DNA sequences corresponding to Arabidopsis XRCC2 and FIGL1 flanked by attB1 and attB2 recombinant tails were cloned into pDONOR221 and pDONOR207, respectively, using the Gateway technology (Thermo Fisher). The fidelity of the coding sequence of all clones was verified by sequencing. The entry vectors were used to generate the appropriate pGAD and pGBK yeast two-hybrid expression vectors. Yeast two-hybrid assays were carried out using a Gal4-based system (Clontech, TakaRabio, Shiga, Japan) by introducing plasmids harboring the gene of

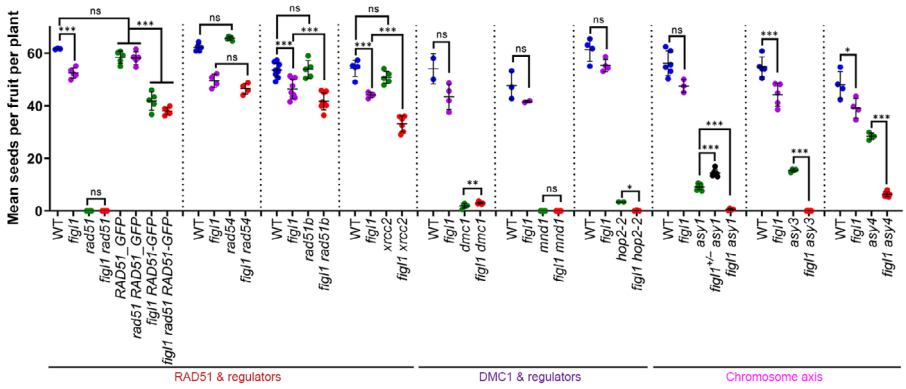

Fig. 1 Comparison of fertility in the *figl1* mutant combined with mutations in genes regulating DMC1/RAD51 or the meiotic chromosome axis in *Arabidopsis thaliana*. Each colored dot represents one plant with the average number of seeds per fruit counted from at least 10 fruits. The mean and the SD are represented by the black bars for each genotype. Each *figl1* double mutant combination is compared with wild-type sister plants and respective single mutants that were cultivated together in a segregating population. Mean and error bars representing SD for each genotype are presented in black. The *P* values shown were computed using an unpaired Kruskal–Wallis test corrected with Dunn's test for multiple comparisons. ns, nonsignificant ($P > 0.01$). *, $P < 0.01$; **, $P < 0.001$; ***, $P < 0.0001$.

interest in yeast strains AH109 and Y187. After mating of haploid yeasts on YPD plates, diploid cells expressing Gal4BD and Gal4AD fusion proteins were selected in SD/LW, a dropout medium without leucine and tryptophan. Protein interactions were assayed by growing diploid cells in serial dilutions for 5 d at 30°C on selective media lacking leucine, tryptophan, histidine, and adenine (SD/LWH and SD/LWHA). Two proteins were deemed to interact when the spots grew on SD-LWH and/or SD-LWHA, and no self-activation could be observed.

Results

Fertility analysis of wild-type and *figl1* plants

We generated numerous genotypes in combination with the *A. thaliana figl1* mutation to study genetic interactions of *FIGL1* during meiotic repair. In all combinations, WT, single, or multiple mutant sister plants were grown together and analyzed. When compared with WT controls, *figl1* mutants showed a slight reduction in fertility (seed set per fruit per plant), which is consistent with the previous report (Fernandes *et al.*, 2018b) and was statistically significant in most genotypes tested, except in a few cases (Fig. 1; Supporting Information Dataset S1). The fertility reduction in *figl1* is correlated with a mild defect in meiotic chromosome segregation due to a shortage of bivalents in 7% of metaphase I cells, as already described (Fernandes *et al.*, 2018a). The remaining genotypes are presented in their respective sections. Briefly, we observed a reduction in fertility when *figl1* was combined with mutations in various regulators of recombinases and the meiotic chromosome axis (Fig. 1; Dataset S1).

Downregulation of RAD51-mediated functions in *figl1* alters meiotic DSB repair outcome

Lack of RAD51 strongly perturbs DMC1-dependent repair (Li *et al.*, 2004). We examined whether the deficiency of both FIGL1 and RAD51 can facilitate DMC1-mediated repair by generating a *figl1 rad51* double mutant. Both *rad51* and *figl1 rad51* showed complete sterility with a mean seed set per fruit of zero (*rad51*: 0 seeds per fruit, no. of plants = 2, no. of fruits = 56; *figl1rad51*: 0 seeds per fruit, no. of plants = 3, no. of fruits = 70) (Fig. 1; Dataset S1). Thus, *rad51* sterility is unchanged in a *figl1* background. Male meiotic progression was also indistinguishable in *rad51* and *figl1 rad51*, with strong chromosome fragmentation indicating unrepaired meiotic breaks (Fig. S1). These observations suggest that *rad51* is epistatic to *figl1* and that loss of FIGL1 and RAD51 together did not facilitate meiotic repair.

We next explored whether or not the RAD51-dependent pathway is necessary for meiotic repair in the absence of FIGL1. Arabidopsis RAD51-GFP is catalytically inactive but can promote DMC1-mediated repair (Cloud *et al.*, 2012; Da Ines *et al.*, 2013b). We combined *figl1* with *rad51 RAD51-GFP* to evaluate whether FIGL1 promotes accurate DMC1-mediated repair in the presence of catalytically inactive RAD51. The fertility of *figl1 rad51 RAD51-GFP* plants (38 seeds per fruit, no. of plants = 5, no. of fruits = 93, corrected Dunn's test $P < 0.0001$) was significantly reduced compared with *figl1* (52 seeds per fruit, no. of plants = 5, no. of fruits = 94) and *rad51 RAD51-GFP* (58 seeds per fruit, no. of plants = 5, no. of fruits = 90) (Fig. 1; Dataset S1) but was similar to *figl1 RAD51-GFP* plants (41 seeds per fruit, no. of plants = 5, no. of fruits = 93, corrected Dunn's test $P > 0.99$) (Fig. 1). This is consistent with the previous observations of *RAD51-GFP* being dominant-negative (Da Ines *et al.*, 2013b). These data demonstrate that mutation in *figl1* significantly reduces fertility in a *RAD51-GFP* background, suggesting that FIGL1 is required to promote DMC1-mediated repair in the absence of a fully functional RAD51.

Cytological analysis of meiotic spreads from male meiocytes revealed a high frequency of metaphase I cells (37%) with univalent pairs in *figl1 rad51 RAD51-GFP* (mean number of bivalents = 4.46, $n = 58$, $P = 0.0001$) compared with 7% of cells in *figl1* (mean number of bivalents = 4.9, $n = 53$) (Fig. 2a,b;

Dataset S2). We hypothesized that the presence of fewer bivalents in *figl1 rad51 RAD51-GFP* could result from a partial defect in the implementation of obligate class I COs in the absence of FIGL1 and catalytically active RAD51. We thus examined the class I CO frequency by immunolocalizing HEI10 and MLH1, which colocalize at class I CO sites in late prophase I as

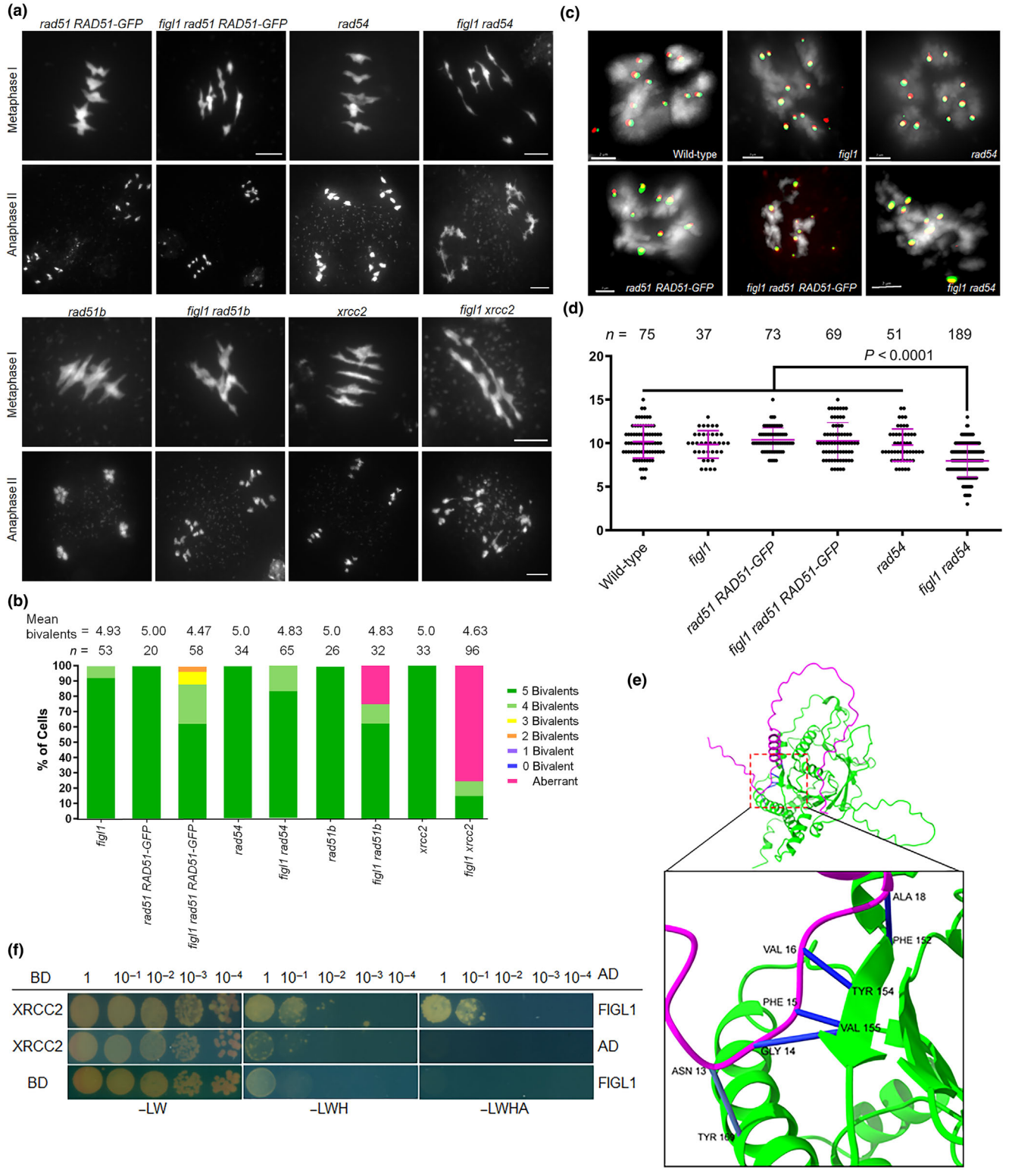

Fig. 2 Downregulation of the RAD51-dependent pathway without FIDGETIN-LIKE-1 (FIGL1) alters meiotic break repair outcomes. (a) Representative metaphase I and anaphase II images of DAPI-stained chromosome spreads of male meiocytes are shown in *rad51b*, *figl1 rad51b*, *xrcc2*, *figl1 xrcc2*, *rad51 RAD51-GFP*, *figl1 rad51 RAD51-GFP*, *rad54*, and *figl1 rad54*. Bars, 5 μm. (b) Quantification of bivalents and aberrant repair in metaphase I. The histograms show the percentage of metaphase cells exhibiting bivalents and chromosome fragmentation. The number of analyzed cells (*n*) and the mean number of bivalents per cell are indicated above each bar. (c) The number of HEI10-MLH1 cofoci is reduced in *figl1 rad54*, but not in *figl1 rad51 RAD51-GFP*. Representative images of HEI10 (red) and MLH1 (green) colocalization in wild-type, *figl1*, *rad54*, *rad51 RAD51-GFP*, *figl1 rad51 RAD51-GFP*, and *figl1 rad54*. Bars, 2 μm. (d) Quantification of HEI10-MLH1 cofoci. Each dot represents a HEI10-MLH1 cofocus in an individual cell, and the red bars represent the mean and SD for each genotype. *n*, number of cells analyzed. The *P* values shown were calculated for unpaired Kruskal–Wallis tests corrected with Dunn's test for multiple comparisons. (e) 3D structure model of interaction between Arabidopsis XRCC2 (in green) and FIGL-FRBD domain (in magenta) by Alphafold2 structural analysis. An enlarged 3D view of the binding interface between XRCC2 and the FIGL1-FRBD domain shows the residues involved. The dark and light blue lines indicate the high confidence predicted aligned error (PAE) scores for residues with < 8 Å distances, as provided by Alphafold2. (f) Yeast two-hybrid assays showing the interaction of Arabidopsis FIGL1 with XRCC2 and DMC1 (used as positive control). Proteins of interest were fused with the Gal4 DNA binding domain (BD, left) and with the Gal4 activation domain (AD, right), respectively, and co-expressed in yeast cells with selection on SD/−LW (− Leu −Trp) for diploid strains and on SD/−LWH (− Leu −Trp −His) as well as SD/−LWHA (− Leu −Trp −His −Ade) for protein interaction.

previously described (Chelysheva *et al.*, 2012). A similar number of HEI10-MLH1 cofoci was observed in *figl1 rad51 RAD51-GFP* (mean = 10.3, n = 189, corrected Dunn's test $P > 0.99$) as in sister WT plants (mean = 10, n = 75), *figl1* and *rad51 RAD51-GFP* (Fig. 2c,d). More univalent pairs with WT levels of MLH1 foci may imply either more intersister repair or defects in CO distribution in *figl1 rad51 RAD51-GFP* compared with *figl1*. In summary, *figl1* does not modulate the number of HEI10-MLH1 cofoci but significantly reduces bivalent formation when RAD51 is catalytically inactive.

Arabidopsis *rad54* mutants show no meiotic defects but display massive chromosome fragmentation in the *rad54 dmc1* mutant, indicating that RAD54 is essential for RAD51-mediated repair in the absence of DMC1 (Hernandez Sanchez-Rebato *et al.*, 2021). We hypothesized that the loss of RAD54 in *figl1* compromises meiotic repair due to its implication in RAD51-mediated repair. We thus tested the epistatic relationship between *rad54* and *figl1*. Fertility of *rad54* (65 seeds per fruit, no. of plants = 5, no. of fruits = 80) compared with the WT (Fig. 1) (62 seeds per fruit, no. of plants = 5, no. of fruits = 82) was not affected as described previously (Hernandez Sanchez-Rebato *et al.*, 2021). The fertility analysis of *figl1 rad54* (46 seeds per fruit, no. of plants = 4, no. of fruits = 70) showed a slightly lower seed set but was not significantly different from *figl1* (49 seeds per fruit, no. of plants = 4, no. of fruits = 67, corrected Dunn's test $P = 0.57$) (Fig. 1). Analysis of meiotic chromosome spreads revealed that *rad54* and the WT displayed 100% metaphase I cells with five bivalents, but *figl1 rad54* showed 16.9% of metaphase cells with univalent pairs compared with 7% cells in *figl1*. The mean number of bivalents per cell in *figl1 rad54* (4.8, n = 65) was not significantly different from that in *figl1* (4.9, n = 53). However, the mean HEI10-MLH1 cofocus formation at late prophase I was *c.* 20% lower in *figl1 rad54* (8 foci, n = 189, corrected Dunn's test $P < 0.0001$) compared with *figl1* (9.9 foci, n = 37), *rad54* (9.8 foci, n = 51), and the WT (10 foci, n = 75) (Fig. 2c,d). These data suggest that the loss of RAD54 activity aggravates *figl1* phenotypes, with a reduced number of HEI10-MLH1 cofoci and an increased number of cells with fewer bivalents. Taken together, our data indicate that the lack of FIGL1 elicits the RAD51-dependent pathway to ensure a WT level of meiotic COs or chiasmata. This relationship may also imply that FIGL1 suppresses the RAD51-dependent repair pathway during WT meiotic repair.

XRCC2 and RAD51B are required for the repair of the meiotic breaks in *figl1*

The cellular activity of RAD51 is regulated by RAD51 paralogs, including RAD51B and XRCC2 (Bleuyard *et al.*, 2005). We examined whether *RAD51B* and *XRCC2* interact genetically with *FIGL1* by analyzing *figl1 rad51b* and *figl1 xrcc2* double mutants for fertility and meiotic defects. Similar to previous observations (Da Ines *et al.*, 2013a; Wang *et al.*, 2014; Hernandez Sanchez-Rebato *et al.*, 2021), the fertility of *rad51b* and *xrcc2* did not differ from their sister WT plants (Fig. 1; Dataset S1). However, both *figl1 rad51b* (42 seeds per fruit, no. of plants = 9, no. of fruits = 56, corrected Dunn's test $P < 0.0001$) and *figl1 xrcc2* (33 seeds per fruit, no. of plants = 6, no. of fruits = 44, corrected Dunn's test $P < 0.0001$) mutants showed lower fertility than *figl1*, and respectively *rad51b* and *xrcc2* (Fig. 1). Thus, loss of FIGL1 affects fertility differentially in *rad51b* and *xrcc2* backgrounds. Our cytological analysis of male meiosis also revealed different severity of meiotic defects. As previously reported, no visible meiotic defects were detected in *rad51b* and *xrcc2* mutants (Da Ines *et al.*, 2013a; Hernandez Sanchez-Rebato *et al.*, 2021). The *figl1 rad51b* mutant displayed 25% metaphase I cells with aberrant chromosome structures and 10% metaphase cells with a mixture of univalents and bivalents, suggesting a defect in meiotic repair (Fig. 2a,b). The *figl1 xrcc2* mutant displayed more severe defects, with 75% of metaphase I cells having chromosome fragmentation, univalents, multivalents, or aberrant structures (Fig. 2a,b). These meiotic catastrophes in both *figl1 rad51b* and *figl1 xrcc2* were also confirmed in subsequent meiotic stages, leading to unbalanced chromosome segregations (Fig. 2a). Altogether, *rad51b* and *xrcc2* do not exhibit any meiotic defects but significantly impair DSB repair in a *figl1* context, revealing that their functional interaction with *FIGL1* promotes meiotic DSB repair.

FIGL1 suppresses partial defects of RAD51 focus formation in *xrcc2* meiocytes

Our data suggested that Arabidopsis XRCC2 and FIGL1 act as positive and negative regulators of RAD51 assembly, respectively. We then explored whether the functional relationship between *XRCC2* and *FIGL1* regulates RAD51 assembly in male meiocytes; to do so, we immunolocalized RAD51 and an axial element (REC8). RAD51 focus formation was observed in WT, *xrcc2*, *figl1*, and *figl1 xrcc2* meiocytes during prophase I, identified by a REC8 signal along the chromosome axis (Fig. 4a). The mean RAD51 focus number was reduced by 27% in *xrcc2* (101 foci, $n = 75$, $P < 0.0001$) compared with WT meiocytes (138 foci, $n = 103$) (Fig. 3a,c). Hence, XRCC2 is required for the formation and/or stabilization of a subset of RAD51 foci during prophase I. Mutation of *figl1* suppressed this partial defect in RAD51 focus formation in *xrcc2*. The *figl1 xrcc2* (254 foci, $n = 75$, $P < 0.0001$) meiocytes showed a significantly higher number of RAD51 foci than *xrcc2* and WT (138 foci, $n = 103$), but similar to *figl1* (204 foci, $n = 89$) (Fig. 3c). These data suggest that FIGL1 disrupts a subset of RAD51 foci in *xrcc2* and that XRCC2 protects RAD51 filaments by partially antagonizing FIGL1 activity during meiosis.

In humans, RAD51 paralogs can protect RAD51 filaments by antagonizing the FIGL1 homolog through protein–protein interaction (Matsuzaki *et al.*, 2019). We therefore tested whether Arabidopsis XRCC2 and FIGL1 also interact. Because XRCC2 has structural similarities with RAD51, which interacts with FIGL1 through FIDGETIN-LIKE-1's RAD51 binding domain (FRBD) (Yuan & Chen, 2013; Fernandes *et al.*, 2018a), we generated an interaction model of XRCC2 and FRBD from FIGL1 using Alphafold2. All five Alphafold2 models predicted a strong interaction with a high interface-predicted template modeling score (ipTM) (> 0.60) and a low predicted aligned error (PAE) value for the FxxA motif in FRBD and three residues of XRCC2 (F152, W154, and V155) (Figs 2e, S2). We also tested the interaction between RAD51B and FRBD using Alphafold2, which did not predict a high ipTM score (< 0.3) compared with the XRCC2 and FRBD interaction (Fig. S2). These observations suggest that XRCC2 likely interacts with FIGL1 through FRBD, more strongly than RAD51B, and that this may be reminiscent of FIGL1 and RAD51 interaction. A yeast two-hybrid assay

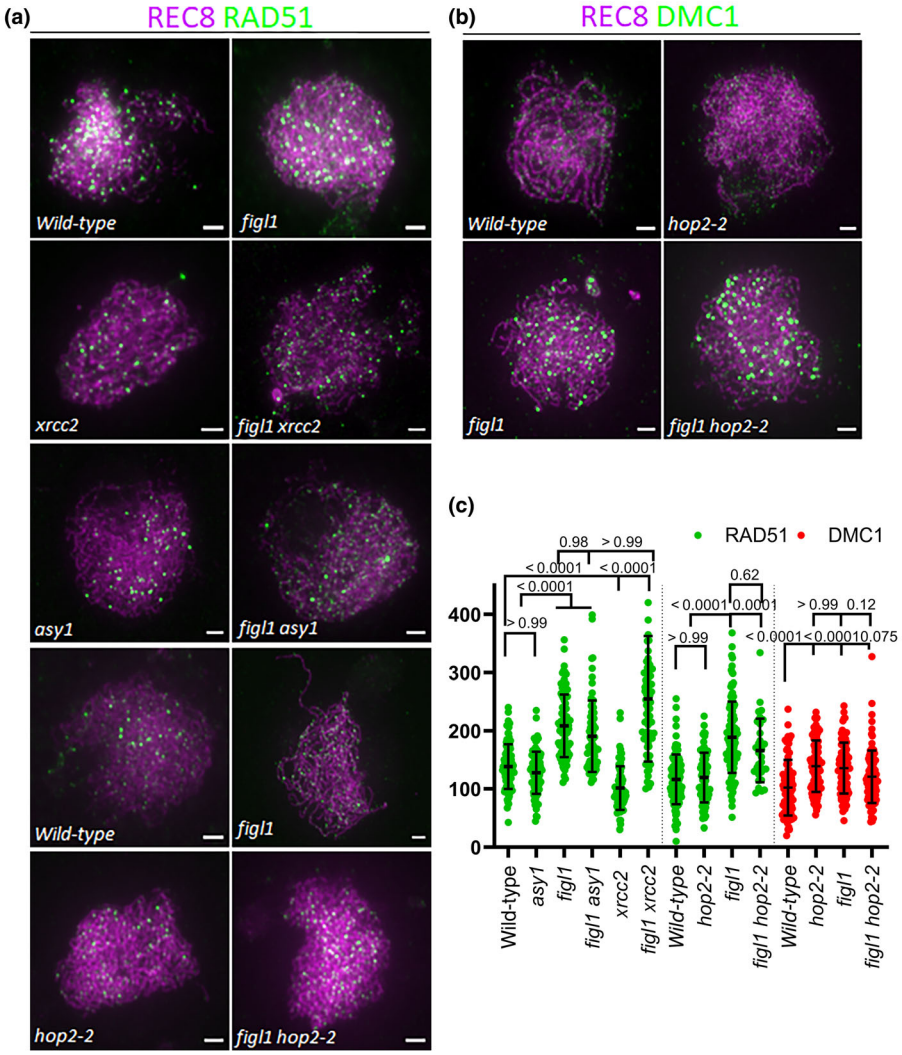

Fig. 3 Analysis of the distribution of RAD51 or DMC1 in various *figl1* mutants. (a) Dual immunolocalization of REC8 (magenta) and RAD51 (green) on male meiocytes from wild-type (WT) (Col-0), *figl1*, *xrcc2*, *figl1 xrcc2*, *asy1*, *figl1 asy1*, and WT, *figl1*, *hop2-2*, *figl1 hop2-2* in the *A. thaliana* Col-0/Ws hybrid background. (b) Dual immunolocalization of REC8 (magenta) and DMC1 (green) in male meiocytes from WT, *figl1*, *hop2-2*, and *figl1 hop2-2* in the Col-0/Ws hybrid background. (c) Quantification of RAD51 and DMC1 foci in different WTs and mutants. The mean and error bars representing SD for each genotype are presented in black. The *P* values shown were calculated using unpaired Kruskal–Wallis tests corrected with Dunn's test for multiple comparisons.

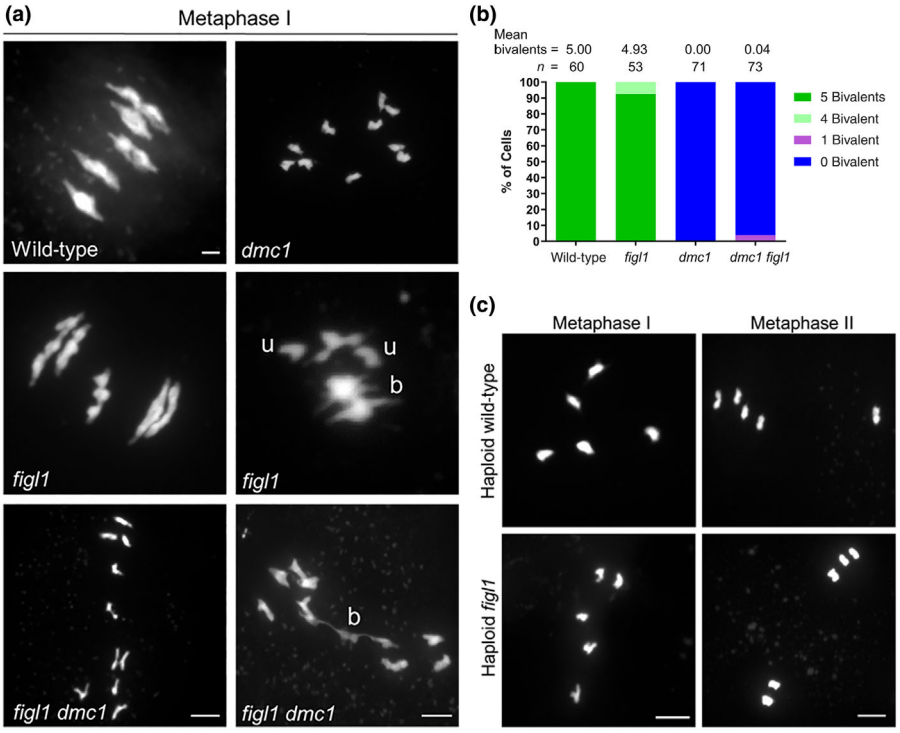

Fig. 4 Chromosome spreads display the completion of meiotic break repair in *A. thaliana* wild-type (WT), *dmc1*, *figl1*, *figl1 dmc1*, and haploid *figl1* mutant plants. (a) Representative metaphase I images of DAPI-stained chromosome spreads of male meiocytes are shown for WT, *figl1*, *dmc1*, and *figl1 dmc1*. b, bivalent or bivalent-like; u, univalent. Bars, 5 μm. Figs 4(a) and 5(a) share the same metaphase image of *figl1* genotype for a direct comparison with other genotypes. (b) Quantification of bivalents at metaphase I. The histogram shows the proportion of cells categorized based on the presence of bivalents. The mean number of bivalents per cell and the number of analyzed cells are indicated above each bar. (c) Metaphase I and II images of DAPI-stained chromosome spreads from haploid WT and *figl1* plants. Bars, 5 μm.

confirmed the interaction between full-length Arabidopsis XRCC2 and FIGL1 (Fig. 2f). These results demonstrate an interaction between XRCC2 and FIGL1 and support the hypothesis that XRCC2 counteracts FIGL1 to protect a subset of RAD51 filaments.

FIGL1 is not necessary for RAD51-dependent repair on sisters in *dmc1* and haploids

RAD51 mediates meiotic DSB repair on sister chromatids in Arabidopsis *dmc1* (Couteau *et al.*, 1999). We explored whether FIGL1 modulates RAD51-mediated meiotic repair without DMC1 by analyzing fertility and male meiosis progression in the *figl1 dmc1* double mutant. The *figl1 dmc1* double mutant was almost sterile with a slightly higher seed set (three seeds per fruit, no. of plants = 6, no. of fruits = 178, corrected Dunn's test $P = 0.001$) than *dmc1* (two seeds per fruit, no. of plants = 5, no. of fruits = 160) (Fig. 1), showing that the *figl1* mutation does not restore fertility but can produce slightly more seeds in a *dmc1* background. Chromosome spreads of male meiocytes revealed that meiotic progression in *figl1 dmc1* was comparable to that in *dmc1*. We detected no pachytene stage with fully coaligned homologous chromosomes in *figl1 dmc1*, similar to *dmc1* (Fig. S3). The *dmc1* mutant displayed 10 univalents in 100% metaphase I cells ($n = 71$) (Fig. 4a), whereas *figl1 dmc1* exhibited 10 univalents in only 96% of metaphase cells ($n = 70$). A lack of chromosome fragmentation at meiosis II indicated DSB repair completion in *figl1 dmc1* (Fig. S3). The remaining 4% metaphase cells ($n = 3$) in *figl1 dmc1* indicated the presence of at least one bivalent (Fig. 4a,b), which may arise from nonhomologous association between homologs or from CO formation between homologous chromosomes. However, we discount the former possibility because such nonspecific associations would not enhance the fertility in *figl1 dmc1* and are absent in *dmc1*. Thus, loss of FIGL1 neither impairs repair on sisters nor restores CO between homologs in *dmc1*, but FIGL1 appears to counteract any rare RAD51-mediated interhomolog repair in the absence of DMC1.

Repairing meiotic breaks relies on RAD51, but not on DMC1 in Arabidopsis haploid meiocytes (Cifuentes *et al.*, 2013), which lack homologs, and the only available repair template is the sister chromatid. We examined whether FIGL1 regulates RAD51-dependent repair on sisters in haploid *figl1*. We analyzed male meiotic progression in Arabidopsis haploid WT and *figl1* plants using chromosome spreads. In WT haploid meiosis, five univalent chromosomes were intact at metaphase I, but segregated unequally at anaphase I and in variable partitioning later in meiosis II (Fig. 4c). Lack of fragmentation suggested efficient repair of meiotic breaks using sister chromatids. No chromosome fragmentation was observed in the *figl1* haploid meiocytes ($n = 32$), and meiosis appeared indistinguishable from the WT (Fig. 4c). Altogether, these results suggest that FIGL1 is not required for RAD51-dependent meiotic DSB repair in haploids or *dmc1* but can suppress rare RAD51-mediated interhomolog invasions.

FIGL1 is indispensable for repair completion in *hop2-2*

DMC1 requires MND1 to facilitate strand invasion on homologs (Kerzendorfer *et al.*, 2006; Panoli *et al.*, 2006). To investigate whether FIGL1 modulates meiotic repair defect when

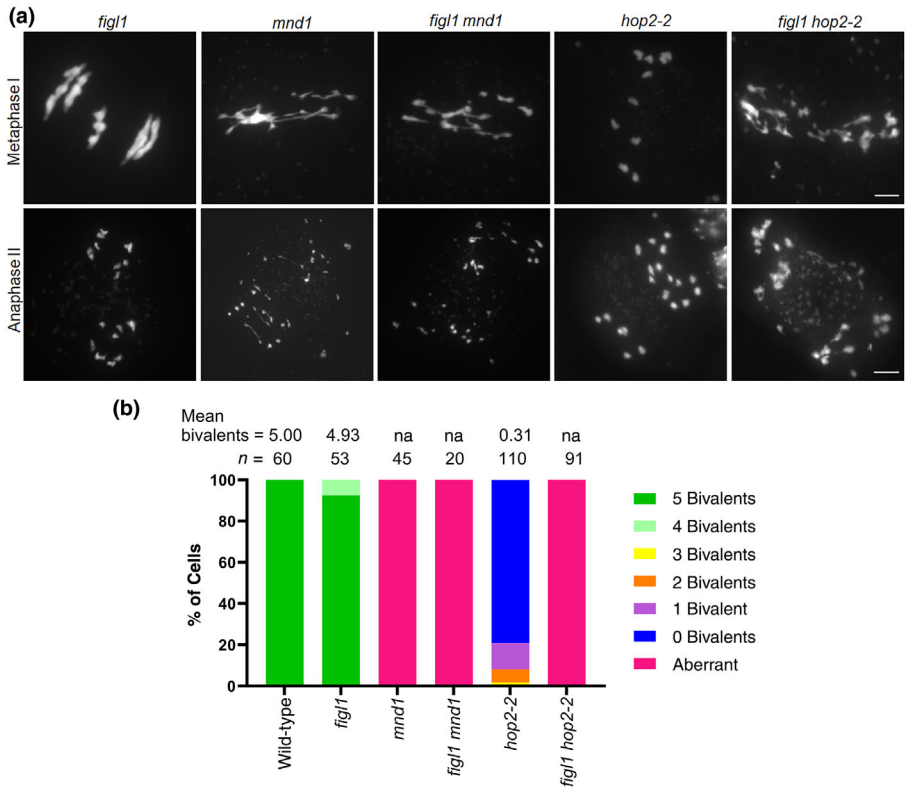

Fig. 5 Epistatic analysis of *A. thaliana mnd1*, *hop2-2*, and *figl1*. (a) Representative metaphase I and anaphase II images of DAPI-stained chromosome spreads of male meiocytes are shown in *figl1*, *mnd1*, *hop2-2*, *figl1 mnd1*, and *figl1 hop2-2*. Bars, 5 μm. Figs 4(a) and 5(a) share the same metaphase image of *figl1* genotype for a direct comparison with other genotypes. (b) Quantification of bivalents and aberrant repair at metaphase I. The histogram shows the proportion of metaphase cells categorized based on the presence of bivalents and chromosome fragmentation. The mean number of bivalents per cell and the number of analyzed cells (*n*) are indicated above each bar. na, not applicable.

DMC1 cannot perform interhomolog invasions in the *mnd1* background, we generated the *mnd1 figl1* mutant. Both *mnd1* (0 seeds per fruit, no. of plants = 4, no. of fruits = 108) and *mnd1 figl1* (0 seeds per fruit, no. of plants = 5, no. of fruits = 86) mutants were fully sterile with empty siliques (Fig. 1), suggesting that *figl1* does not alter the fertility of *mnd1*. Similar to previous observations (Kerzendorfer *et al.*, 2006), analysis of male *mnd1* meiocyte spreads showed no pachytene cells with synapsed chromosomes and strong chromosome fragmentation at meiosis I and II (Fig. 5a). This observation supports a lack of interhomolog strand invasion and unrepaired breaks in *mnd1*. The double *mnd1 figl1* also showed meiotic progression with chromosome fragmentation, which was indistinguishable from *mnd1* (Fig. 5a), indicating that *mnd1* is epistatic to *figl1*.

The *hop2-2* hypomorphic mutation weakly supports DMC1 functions that lead to the RAD51-dependent DSB repair on sisters and severely disrupt interhomolog repair (Uanschou *et al.*, 2014). We investigated whether FIGL1 is involved in meiotic repair when DMC1 is not fully active by analyzing the *figl1 hop2-2* double mutant. The fertility of *figl1 hop2-2* plants (0.1 seeds per fruit, no. of plants = 3, no. of fruits = 64, corrected Dunn's test $P = 0.0049$) was lower than in *hop2-2* (three seeds per fruit, no. of plants = 2, no. of fruits = 40), WT (62 seeds per fruit, no. of plants = 4, no. of fruits = 76, corrected Dunn's test $P < 0.0001$), and *figl1* (54 seeds per fruit, no. of plants = 3, no. of fruits = 75, corrected Dunn's test $P < 0.0001$) (Fig. 1; Dataset S1). Cytological analysis of metaphase I from male *figl1 hop2-2* meiocytes further corroborated the reduction in fertility with defects in meiotic progression (Fig. 5a). As reported previously (Uanschou *et al.*, 2014), we detected only 20% of metaphase I cells with 1–3 bivalents, the rest having only univalent chromosomes in male *hop2-2* meiocytes (Fig. 5b). In *figl1 hop2-2*, all metaphase I cells ($n = 91$) and subsequent meiotic stages exhibited strong chromosome fragmentation compared with the *hop2-2* meiocytes (Fig. 5a). These results indicate that *figl1* strongly disrupts meiotic repair in *hop2-2* and implies that FIGL1 is involved in meiotic repair switching from interhomolog to mostly intersister when DMC1 is partially active.

We then examined whether meiotic repair defects in *figl1 hop2-2* could be explained by hyperaccumulation of both recombinases during prophase I. To do so, we immunolocalized RAD51 or DMC1 with the axial element (REC8) and the transverse filament protein of the SC (ZYP1) in male meiocytes. Average RAD51 foci per cell during prophase I did not differ between WT (foci = 115, $n = 104$) and *hop2-2* (foci = 114, $n = 76$) meiocytes but were significantly higher in *figl1 hop2-2* (foci = 155, $n = 31$) and *figl1* (foci = 186, $n = 116$) (Fig. 3a,c). A marked increase in mean DMC1 foci per cell was observed in *hop2-2* (foci = 138, $n = 93$) meiocytes relative to WT (foci = 101, $n = 74$) but was similar to *figl1* (foci = 135, $n = 93$) and *figl1 hop2-2* (foci = 120, $n = 100$) (Fig. 3b,c). These observations suggest that FIGL1 does not alter the number of DMC1 foci but appears to suppress RAD51 focus formation in *hop2-2*. We have previously shown that *figl1* mutation restores RAD51 and DMC1 focus formation and suppresses defects in

synapsis between homologs in *brca2a brca2b* and *sds* (Fernandes *et al.*, 2018a; Kumar *et al.*, 2019). Because no pachytene was observed in *hop2-2* suggesting a defective synapsis, we investigated whether synapsis was restored partially or fully in *figl1 hop2-2* using ZYP1 immunostaining. Only punctuated ZYP1 signals were observed in *figl1 hop2-2* relative to *hop2-2*, while WT and *figl1* meiocytes showed continuous ZYP1 signal along the entire length of chromosomes (Fig. S4). These results imply that overaccumulation of RAD51 and DMC1 foci does not restore interhomolog invasion in *figl1 hop2-2* and that FIGL1 likely promotes meiotic repair in *hop2-2* by suppressing RAD51 foci.

FIGL1 promotes meiotic repair in *asy1*, *asy3*, and *asy4* with impaired interhomolog bias

We further explored whether FIGL1 is critical for meiotic repair when both RAD51 and DMC1 are active, but interhomolog bias is impaired. Unlike in *hop2-2*, DMC1 is proficient for meiotic repair in *asy1*, *asy3*, and *asy4* mutants, which lack full synapsis, have no pachytene stage, and show reduced bivalent formation (Sanchez-Moran *et al.*, 2007; Ferdous *et al.*, 2012; Chambon *et al.*, 2018). *asy1* is epistatic over *asy3* and *asy4*, and shows the lowest number of bivalents in metaphase I followed by *asy3* and *asy4* (Ferdous *et al.*, 2012; Chambon *et al.*, 2018). The reduction in interhomolog COs, no fragmentation, and fewer bivalent numbers suggest that most meiotic DSBs are efficiently repaired on sisters instead of homologs in *asy* mutants. We generated *figl1 asy1*, *figl1 asy3*, and *figl1 asy4* double mutants and analyzed fertility and meiotic defects. All three single mutants, *asy1* (10 seeds per fruit, no. of plants = 2, no. of fruits = 23), *asy3* (15 seeds per fruit, no. of plants = 3, no. of fruits = 83), and *asy4* (28 seeds per fruit, no. of plants = 4, no. of fruits = 80), showed a severe reduction in fertility, albeit to a variable extent, compared with *figl1* (44 seeds per fruit, no. of plants = 5, no. of fruits = 100) and the WT (54 seeds per fruit, no. of plants = 5, no. of fruits = 100). Both *figl1 asy1* and *figl1 asy3* double mutants were sterile and barely produced any seeds (*figl1 asy1*: 0.6 seeds per fruit, no. of plants = 4, no. of fruits = 70, corrected Dunn's test $P < 0.0001$; *figl1 asy3*: 0 seeds per fruit, no. of plants = 7, no. of fruits = 138, corrected Dunn's test $P < 0.0001$) (Fig. 1; Dataset S1). The *figl1 asy4* plants produced a few seeds, but fertility was decreased by more than fourfold (six seeds per fruit, no. of plants = 7, no. of fruits = 140, corrected Dunn's test $P < 0.0001$), relative to *asy4* and *figl1* (Fig. 1; Dataset S1). Intriguingly, the fertility of *figl1/+ asy1* (14 seeds per fruit, no. of plants = 6, no. of fruits = 95, corrected Dunn's test $P < 0.0001$) was significantly higher than in *asy1* (nine seeds per fruit, no. of plants = 8, no. of fruits = 106), and no significant difference in fertility was observed in *figl1/+ asy3* (20 seeds per fruit, no. of plants = 6, no. of fruits = 60, corrected Dunn's test $P = 0.074$) and *asy3* (15 seeds per fruit, no. of plants = 9, no. of fruits = 133), suggesting that meiotic repair is sensitive to FIGL1 dosage in *asy1*. In summary, the *figl1* mutation marginally affects fertility in the WT context, but it strongly reduces fertility in *asy1*, *asy3*, and *asy4* mutants of meiotic axis components.

Further, nuclear spread analysis of male meiocytes in *asy1*, *asy3*, and *asy4* showed mean bivalent numbers of 1.66 ($n = 50$), 3.0 ($n = 67$), and 4.1 ($n = 38$) at metaphase I, respectively (Fig. 6). These values confirmed the previous observations of *asy1* being most affected in CO formation (Sanchez-Moran *et al.*, 2007; Ferdous *et al.*, 2012; Chambon *et al.*, 2018). The *figl1 asy1* mutants exhibited 82% of aberrant metaphases ($n = 52$) with unrepaired meiotic breaks, which was never observed in *figl1* or *asy1* (Fig. 6a,b). We, however, detected a fraction of nonaberrant metaphase cells (18%) without any fragmentation, but showing a mixture of univalent and bivalent chromosomes with a higher mean number of bivalents per cell (3.22, $n = 10$) compared with *asy1*. These results indicate that *figl1* not only strongly impairs meiotic repair in most *asy1* meiocytes but also partially restores bivalent formation between homologs in a fraction of meiocytes and provide evidence that FIGL1 suppresses interhomolog repair in *asy1*. We, therefore, analyzed whether the reduction in FIGL1 dosage increases bivalent formation in *figl1/+ asy1*. The *figl1/+ asy1* mutant showed a significantly higher mean number of bivalents per cell (2.5, $n = 52$) in metaphase I cells than in *asy1*. These observations offer further support that FIGL1 attenuates interhomolog repair when lacking *asy1* and suggest that ASY1 counteracts FIGL1 to promote interhomolog repair.

Although *asy3* is less affected than *asy1*, the *figl1 asy3* exhibited the most severe meiotic defect of 100% aberrant metaphases ($n = 86$) with chromosome fragmentation, indicating that FIGL1 is essential for meiotic repair in *asy3* (Fig. 6). The *figl1 asy4* mutants, however, displayed the least severe meiotic defects among the three *figl1 asy* mutants, with 75% of metaphase cells showing a lower mean bivalent number per cell in *figl1 asy4* (3.13, $n = 56$) than in *asy4* (4.1, $n = 38$) (Fig. 6). The remaining 25% metaphase cells in *figl1 asy4* were aberrant with unrepaired breaks (Fig. 6a,b). Meiotic defects in all three *figl1 asy* double mutants were also detected at the postmetaphase I stages, showing chromosome fragmentation, bridges, and unbalanced chromosomal segregation (Fig. 6a). In summary, *figl1* severely impairs meiotic repair in the *asy1*, *asy3*, and *asy4* mutants affected in interhomolog bias and appears to enhance interhomolog repair in *asy1*.

We further assessed whether the repair defects in *figl1 asy1* led to a change in RAD51 focus formation by immunolocalizing RAD51 and REC8 in male meiocytes. Similar to previous observations (Sanchez-Moran *et al.*, 2007), the number of RAD51 foci was not different in *asy1* (foci = 127, $n = 94$) and WT meiocytes (foci = 138, $n = 103$) (Fig. 3). As expected, both *figl1* (foci = 208, $n = 89$) and *figl1 asy1* (foci = 190, $n = 73$) showed a significant increase in RAD51 foci compared with *asy1* and the WT but did not differ from each other. These observations indicate that FIGL1 limits overaccumulation of RAD51 foci in *asy1* to promote meiotic repair. However, the outcomes of RAD51 foci accumulation in *figl1* and *figl1 asy1* differ because repair is carried out to completion in *figl1*, but not in *figl1 asy1*.

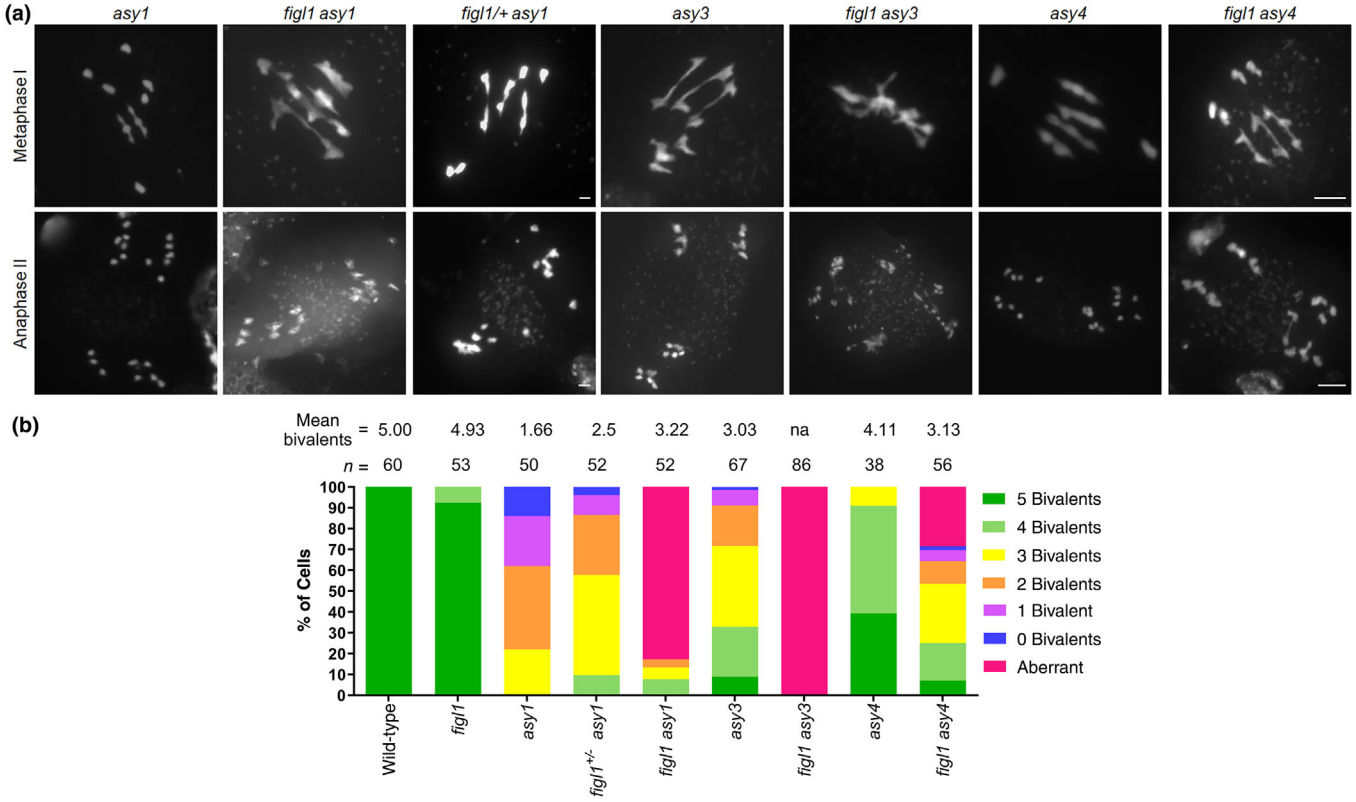

Fig. 6 Functional interaction of *A. thaliana figl1* with *asy1*, *asy3*, and *asy4*. (a) Representative metaphase I and anaphase II images of DAPI-stained chromosome spread of male meiocytes are shown in *asy1*, *asy3*, *asy4*, *figl1 asy1*, *figl1/+ asy1*, *figl1 asy3*, and *figl1 asy4*. Bars, 5 μm. (b) Quantification of bivalents and aberrant repair at metaphase I. The proportion of metaphase cells categorized based on the presence of bivalents and chromosome fragmentation is presented. The mean number of bivalents per cell and the number of analyzed cells (*n*) are indicated above each bar. na, not applied.

Discussion

RAD51-dependent repair in *figl1* is critical for correct meiotic repair outcome

Our data indicate a functional association between FIGL1 and the RAD51-dependent repair pathway during meiosis. The RAD51 pathway is critical for repairing DSBs before/at meiotic entry and in late prophase I (Crismani *et al.*, 2013; Joshi *et al.*, 2015; Enguita-Marruedo *et al.*, 2019), providing an alternative to the DMC1-dependent pathway. However, simultaneous activation of Dmc1 and Rad51 in budding yeast elicits distinct factors and increases the time it takes to repair Rad51-mediated interhomolog intermediates (Ziesel *et al.*, 2022). Arabidopsis *figl1* mutants display a change in kinetics, with massive accumulation of RAD51 foci on meiotic chromosomes until late pachytene compared with WT meiocytes (Fernandes *et al.*, 2018a). We speculated that RAD51, in addition to DMC1, is active for interhomolog invasions, leading to aberrant recombination intermediates in *figl1*. These intermediates require MUS81 endonuclease activity that becomes necessary for repair completion in *figl1 mus81* (Girard *et al.*, 2015; Kumar *et al.*, 2019). FIGL1 is, however, essential for meiotic DSB repair in various crop plants, in which the *figl1* mutant shows chromosome fragmentation in metaphase I (Zhang *et al.*, 2017; Yang *et al.*, 2022; Osman *et al.*, 2024). These unrepaired breaks may result from complex DMC1- and RAD51-mediated interhomolog invasions that MUS81 may be unable to repair (Mu *et al.*, 2023). Here, our data provide evidence that the RAD51-dependent pathway promotes accurate meiotic repair outcomes in Arabidopsis *figl1*. First, the inhibition of RAD51 catalytic activity in *figl1* results in a higher percentage of metaphase cells with univalents, albeit with WT levels of HEI10-MLH1 cofoci during prophase I. This suggests either a defect in CO distribution or COs forming between sister chromatids in *figl1 rad51 RAD51-GFP*. Second, downregulation of RAD54, which impairs RAD51-dependent repair, is required to maintain the WT level of HEI10-MLH1 cofoci as judged from the *c.* 20% reduction in *figl1 rad54*. Third, the loss of RAD51B or XRCC2 leads to unrepaired breaks in *figl1 rad51b* and *figl1 xrcc2*, indicating that the RAD51-dependent pathway becomes limiting for recombination when lacking FIGL1. Thus, it is tempting to speculate that FIGL1 suppresses RAD51-dependent interhomolog repair to limit class II COs (Fig. 7) and to regulate class I CO distribution in WT meiosis in Arabidopsis.

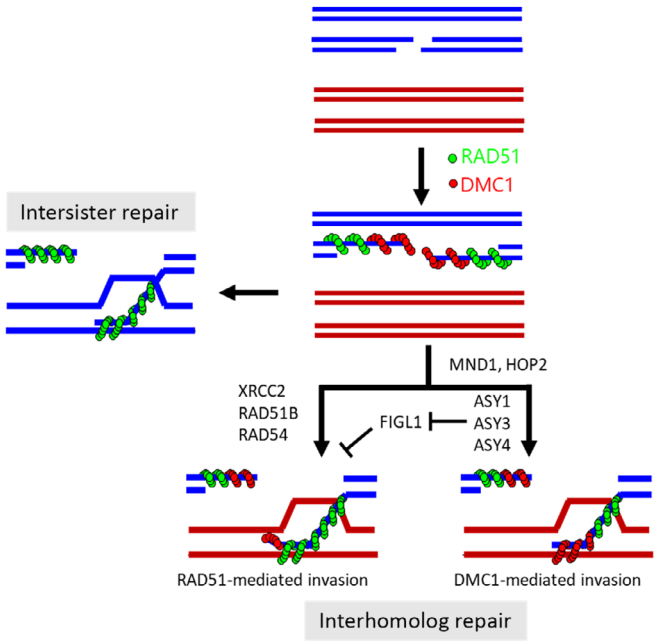

Fig. 7 Model for FIDGETIN-LIKE-1 (FIGL1) *in vivo* functions during meiotic break repair in *A. thaliana*. Blue and red lines represent homologous chromosomes, and four lines in the same color denote the two DNA strands of each sister chromatid. After the formation of double-stranded breaks (DSB) and the resection of 5′ ends, RAD51 and DMC1 polymerize at 3′ single-strand DNA (ssDNA) tails to form nucleoprotein homofilaments. DMC1 is proximal to the DSB site, but RAD51 is distal to the DSB site. Invasion of these homofilaments leads to the repair of meiotic breaks. FIGL1 can negatively regulate RAD51 and DMC1 activity at pre- and postinvasion steps. FIGL1 is not required for RAD51-mediated intersister repair of meiotic breaks in the absence of DMC1 in plants. However, FIGL1 can antagonize RAD51-mediated interhomolog invasions in the presence of DMC1. MND1 and HOP2 likely act upstream of FIGL1. The three meiotic axis proteins (ASY1, ASY3, and ASY4) act as positive modulators of interhomolog recombination by counteracting FIGL1 activity. In the absence of FIGL1, RAD51 is likely active for interhomolog invasions/repair in XRCC2 and RAD51B-dependent manner. RAD54 and the catalytic activity of RAD51 are critical for ensuring the wild-type level or distribution of meiotic CO/chiasmata formation when lacking FIGL1.

Arabidopsis XRCC2 partially counteracts FIGL1 to promote RAD51-dependent repair

The roles of Arabidopsis RAD51B, RAD51D, and XRCC2 during meiosis have remained enigmatic despite the proposed early and late roles of these RAD51-mediators in other plant species (Charlot *et al.*, 2014; Zhang *et al.*, 2020; F. Zhang *et al.*, 2023). The absence of any obvious meiotic defects in single, double, and triple mutants of Arabidopsis *RAD51B*, *RAD51D*, and *XRCC2* indicates that they are not essential for DMC1-mediated repair during meiosis (Bleuyard *et al.*, 2005; Wang *et al.*, 2014; Hernandez Sanchez-Rebato *et al.*, 2021). Mutants of *rad51b*, *rad51d*, and *xrcc2*, when combined with *dmc1*, have no impact on meiosis, suggesting that they are not necessary for RAD51-mediated repair on sisters (Hernandez Sanchez-Rebato *et al.*, 2021). However, an increase in meiotic COs between homologs in Arabidopsis *xrcc2* and *rad51b* remains unexplained (Da Ines *et al.*, 2013a). Our findings demonstrate a genetic interaction between *xrcc2*, *rad51b* and *figl1*, with the latter playing a critical role in meiotic DSB repair. First, both *figl1 rad51b* and *figl1 xrcc2* mutants have severe meiotic defects, although in varying degrees. These defects indicate that both paralogs are necessary for repairing meiotic breaks when FIGL1 is absent, with the loss of XRCC2 producing more severe meiotic defects. Recent structural studies of the human BCDX2 complex have suggested that the RAD51 ensemble interacts with the BCDX2 complex by engaging with RAD51B, but not with XRCC2 (Greenhough *et al.*, 2023; Rawal *et al.*, 2023). We speculate that the BCD complex can still engage with RAD51-filaments through RAD51B, leading to more toxic recombination intermediates and severe meiotic defects in *figl1 xrcc2*, compared with no interaction of the CDX2 complex in *rad51b* with the RAD51 ensemble. Second, we observed a decrease in RAD51 focus number in the *xrcc2* meiocytes compared with the WT and an increase in RAD51 focus number in *figl1 xrcc2* and *figl1*. This pattern suggests that XRCC2 stabilizes or protects a subset of RAD51 filaments from the destabilizing activity of FIGL1, arguing for partial antagonism between XRCC2 and FIGL1. We also detected a protein–protein interaction between XRCC2 and FIGL1, which is consistent with the model wherein the interaction of RAD51 paralogs counteracts the destabilizing functions of FIGL1 or other negative regulators (Liu *et al.*, 2011; Matsuzaki *et al.*, 2019). We speculate that XRCC2 counteracts FIGL1 activity from the nonengaging end of BCDX2 complex and acts, in addition to BRCA2, at the postnucleofilament assembly step during meiosis.

Furthermore, our data also suggest that when both RAD51 and DMC1 are active for homolog invasions (Fig. 7), the RAD51-dependent repair pathway has additional requirements compared with those when DMC1 is absent or not functioning. One possibility is that XRCC2 and RAD51B are needed to process a subset of RAD51-mediated invasions, especially in *figl1*, when RAD51 is probably blocked from polymerizing to 3′ ends (Fig. 7). XRCC2 can also promote the processing of the recombination intermediates through its interaction with RAD51D to form a subcomplex (DX2) (Thacker, 2005), which can recruit additional factors (Braybrooke *et al.*, 2003; F. Zhang *et al.*, 2023). Altogether, our data indicate that Arabidopsis XRCC2 and RAD51B promote RAD51-dependent repair during meiosis.

ASY1 counteracts FIGL1 activity to promote interhomolog recombination

Arabidopsis ASY1, ASY3, and ASY4 are three meiotic axis proteins whose mechanism in interhomolog repair remains elusive. ASY1 appears to be a main player as judged from the lowest chiasma level and epistatic analysis among *asy* mutants (Chambon *et al.*, 2018). The lack of ASY1 does not affect total MLH1 focus numbers, but 50% occur between sister chromatids, indicating reduced interhomolog and high intersister recombination levels in *asy1* (Lambing *et al.*, 2020). ASY1 stabilizes DMC1 onto DSBs without affecting RAD51 localization (Sanchez-Moran *et al.*, 2007). The residual interhomolog recombination in *asy1*

still depends on DMC1 because the *asy1 dmc1* mutant shows only univalents with DSBs repaired by RAD51 using sisters (Sanchez-Moran *et al.*, 2007). Thus, the loss of ASY1 activates both the RAD51- and the DMC1-dependent pathways to repair meiotic breaks. Our findings show that FIGL1 is required to maintain the balance between interhomolog and intersister recombination f or repair completion in *asy1*. The *figl1 asy1* is completely sterile, and 82% of metaphase I cells exhibit an aberrant phenotype with DNA fragmentation. We noticed that 18% metaphase I cells showed no fragmentation but had a significantly higher mean number of bivalents (3.22) in *figl1 asy1* than in *asy1* (1.66 bivalents) (Fig. 6). Furthermore, the reduction in FIGL1 dosage in *figl/+ asy1* also led to an increase in mean bivalent number as well as a higher mean seed set per fruit compared with *asy1* (Figs 1, 6). This indicates that FIGL1 suppresses interhomolog invasion in the absence of ASY1, and the repair defects in *figl1 asy1* can thus be attributed to an increase in interhomolog invasions. Altogether, ASY1 counteracts FIGL1 activity to promote interhomolog recombination.

Our data also indicate a functional relationship between *asy3*, *asy4*, and *figl1* for the completion of meiotic break repair. The double mutant *figl1 asy3* exhibited the most severe repair defect phenotype due to the presence of chromosome fragmentation in 100% of metaphase I (Fig. 6). The absence of ASY3 significantly changes the localization of ASY1, which forms foci instead of linear structures and reduces the level of DSBs, as measured by proxy based on the number of RAD51 and DMC1 foci in *asy3* (Ferdous *et al.*, 2012). One attractive hypothesis is that chromosome fragmentation defects result from interhomolog invasion imposed by altered ASY1 localization, along with deregulation of RAD51/DMC1 dynamics in *figl1 asy3*. However, the double *figl1 asy4* mutant showed less severe repair defects with only 25% of aberrant metaphase I cells and an overall mean number of bivalents reduced to 2.84. ASY1 and ASY3 are recruited in *asy4*, but form abnormal patchy and lumpy patterns on the chromosome axis; furthermore, ASY1 is not depleted from the synapsed regions (Chambon *et al.*, 2018). We suspect that the presence of ASY1 and ASY3 in *figl1 asy4* enforces interhomolog invasions and counteracts FIGL1 functions up to a certain extent, resulting in partly unrepaired breaks and defects in chiasma formation. In our model (Fig. 7), ASY proteins act as positive modulators of interhomolog recombination, while FIGL1 counteracts interhomolog invasions. Lack of both FIGL1 and ASY proteins would thus lead to aberrant meiotic DSB repair.

Arabidopsis FIGL1 promotes meiotic intersister repair when interhomolog bias is impaired

In plants, RAD51 repairs meiotic DSBs using sister chromatids in *dmc1* (Couteau *et al.*, 1999; Wang *et al.*, 2016), suggesting either plant RAD51 is unable to perform interhomolog invasions or RAD51-mediated interhomolog invasions in *dmc1* can be actively counteracted by an unknown factor(s). Our data show that FIGL1 does not modulate RAD51-mediated intersister repair in *dmc1* or haploid meiosis. We observed univalents and no fragmentation in *Arabidopsis figl1 dmc1* and haploid *figl1* mutants (Fig. 2). However, we noticed the presence of rare bivalents and slightly higher fertility in *figl1 dmc1* compared with *dmc1*. This observation favors the idea that RAD51 mediates interhomolog invasions at a low frequency in *dmc1* and that FIGL1 counteracts these interhomolog invasions in *dmc1*.

DMC1 is crucial for interhomolog bias, and its dysfunction leads to weakened interhomolog bias in *hop2-2* and *asy1* (Sanchez-Moran *et al.*, 2007; Uanschou *et al.*, 2014; Lambing *et al.*, 2020). The insufficient amount of functional HOP2/MND1 complexes results in a majority of univalents and rare, DMC1-dependent bivalents (*c.* 0.5 per cell) at metaphase I in *hop2-2* (Uanschou *et al.*, 2014). Similarly, most univalents and a few DMC1-dependent bivalents (*c.* 1.7 per cell) were observed when the stability of DMC1 was compromised in *asy1*. DMC1 dysfunction thus leads to more repair on sisters at the expense of lower interhomolog repair in *hop2-2* and *asy1*. We found that FIGL1 is critical for this shift in meiotic DSB repair in *hop2-2* and *asy1*. How does FIGL1 shift repair between interhomolog and intersister? Our data show a hyperaccumulation of RAD51 foci in *figl1 hop2-2* and *figl1 asy1* meiocytes, compared with *hop2-2* and *asy1*, but similar to *figl1*. This pattern of hyperaccumulation indicates that RAD51 foci accumulation largely depends on FIGL1 and is likely independent of HOP2 and ASY1. Because FIGL1 is not necessary for intersister repair (in *dmc1*) but counteracts interhomolog invasions (in *asy1* and *dmc1*), our data imply that FIGL1 dismantles a subset of RAD51 filaments, in addition to DMC1 filaments, arising from interhomolog invasions in *hop2-2* and *asy1* to promote repair on sisters. The strong fragmentation observed in *figl1 hop2-2* and *figl1 asy1*, but not in *figl1*, also suggests that HOP2 and ASY1 promote DSB repair in *figl1*. We speculate that an interplay between HOP2, ASY1, and FIGL1 is required for WT levels of interhomolog recombination in Arabidopsis. Unlike the antagonism between BRCA2 or SDS and FIGL1 at the nucleofilament formation step, we propose that ASY1 counteracts FIGL1 activity for a subset of recombinase foci at postinvasion steps.

Conclusions

In conclusion, the genetic interactions of *figl1* revealed that FIGL1 attenuates interhomolog repair during meiosis and that these genetic interactions are an essential determinant of the meiotic break repair outcome. We have previously shown that BRCA2 and SDS antagonize FIGL1 activity to protect RAD51/DMC1 foci, likely at the step of nucleofilament formation. This study suggests that multiple factors can counteract FIGL1 activity, in addition to BRCA2 and SDS, likely at the invasion step after nucleofilament formation to promote meiotic interhomolog repair.

Acknowledgements

We are grateful to Christine Mezard and Mathilde Grelon for fruitful discussions and critical reading of the manuscript. We also thank Christine Mezard for the technical help in generating Alphafold2 models. We thank Oliver Da Ines for the XRCC2

construct and rabbit anti-DMC1 antibodies. This work was supported by the ANR-FIRE funding (ANR-17-CE12-0015) to RM and RK. RK also received a financial support from La Ligue Contre le Cancer. CE was supported by Rijk Zwaan Zaadteelt en Zaadhandel B.V., Burgemeester Crezeelaan 40, 2678 KX, De Lier. This work has benefited from the support of IJPB's Plant Observatory technological platforms. The IJPB benefits from the support of LabEx Saclay Plant Sciences-SPS (ANR-10-LABX-0040-SPS).

Competing interests

None declared.

Author contributions

CE, SP, FT, JG, AH, AC and CG produced the data. CE, CG, RM and RK analyzed the data. RK and RM conceived and designed the experiments. CE and RK wrote the manuscript with the input of all authors.

ORCID

Aurélie Chambon https://orcid.org/0000-0003-2984-2108
Côme Emmenecker https://orcid.org/0009-0002-4406-5327
Chloé Girard https://orcid.org/0000-0002-1459-6226
Aurélie Hurel https://orcid.org/0000-0002-6416-4392
Rajeev Kumar https://orcid.org/0000-0002-3895-8164
Raphael Mercier https://orcid.org/0000-0001-6508-6608

Data availability

The data that support the findings of this study are available in the Supporting Information of this article (Datasets S1, S2).

References

Abe K, Osakabe K, Nakayama S, Endo M, Tagiri A, Todoriki S, Ichikawa H, Toki S. 2005. Arabidopsis RAD51C gene is important for homologous recombination in meiosis and mitosis. *Plant Physiology* **139**: 896–908.

Armstrong SJ, Caryl AP, Jones GH, Franklin FCH. 2002. Asy1, a protein required for meiotic chromosome synapsis, localizes to axis-associated chromatin in Arabidopsis and Brassica. *Journal of Cell Science* **115**: 3645–3655.

Azumi Y. 2002. Homolog interaction during meiotic prophase I in Arabidopsis requires the SOLO DANCERS gene encoding a novel cyclin-like protein. *EMBO Journal* **21**: 3081–3095.

Berchowitz LE, Francis KE, Bey AL, Copenhaver GP. 2007. The role of AtMUS81 in interference-insensitive crossovers in *A. thaliana*. *PLoS Genetics* **3**: e132.

Bishop DK. 1994. RecA homologs Dmc1 and Rad51 interact to form multiple nuclear complexes prior to meiotic chromosome synapsis. *Cell* **79**: 1081–1092.

Bleuyard J-Y, Gallego ME, Savigny F, White CI. 2005. Differing requirements for the Arabidopsis Rad51 paralogs in meiosis and DNA repair. *The Plant Journal* **41**: 533–545.

Bleuyard J-Y, White CI. 2004. The Arabidopsis homologue of Xrcc3 plays an essential role in meiosis. *EMBO Journal* **23**: 439–449.

Braybrooke JP, Li J-L, Wu L, Caple F, Benson FE, Hickson ID. 2003. Functional interaction between the Bloom's syndrome helicase and the RAD51 paralog, RAD51L3 (RAD51D). *Journal of Biological Chemistry* **278**: 48357–48366.

Brown MS, Bishop DK. 2014. DNA strand exchange and RecA homologs in meiosis. *Cold Spring Harbor Perspectives in Biology* **7**: a016659.

Brown MS, Grubb J, Zhang A, Rust MJ, Bishop DK. 2015. Small Rad51 and Dmc1 complexes often co-occupy both ends of a meiotic DNA double strand break. *PLoS Genetics* **11**: e1005653.

Busygina V, Sehorn MG, Shi IY, Tsubouchi H, Roeder GS, Sung P. 2008. Hed1 regulates Rad51-mediated recombination via a novel mechanism. *Genes & Development* **22**: 786–795.

Callender TL, Laureau R, Wan L, Chen X, Sandhu R, Laljee S, Zhou S, Suhandynata RT, Prugar E, Gaines WA *et al.* 2016. Mek1 down regulates Rad51 activity during yeast meiosis by phosphorylation of Hed1. *PLoS Genetics* **12**: e1006226.

Caryl AP, Armstrong SJ, Jones GH, Franklin FC. 2000. A homologue of the yeast HOP1 gene is inactivated in the Arabidopsis meiotic mutant asy1. *Chromosoma* **109**: 62–71.

Chambon A, West A, Vezon D, Horlow C, De Muyt A, Chelysheva L, Ronceret A, Darbyshire A, Osman K, Heckmann S *et al.* 2018. Identification of ASYNAPTIC4, a component of the meiotic chromosome axis. *Plant Physiology* **178**: 233–246.

Chan Y-L, Brown MS, Qin D, Handa N, Bishop DK. 2014. The third exon of the budding yeast meiotic recombination gene HOP2 is required for calcium-dependent and recombinase Dmc1-specific stimulation of homologous strand assimilation. *Journal of Biological Chemistry* **289**: 18076–18086.

Charlot F, Chelysheva L, Kamisugi Y, Vrielynck N, Guyon A, Epert A, Le Guin S, Schaefer DG, Cuming AC, Grelon M *et al.* 2014. RAD51B plays an essential role during somatic and meiotic recombination in *Physcomitrella*. *Nucleic Acids Research* **42**: 11965–11978.

Chelysheva L, Grandont L, Vrielynck N, le Guin S, Mercier R, Grelon M. 2010. An easy protocol for studying chromatin and recombination protein dynamics during *Arabidopsis thaliana* meiosis: immunodetection of cohesins, histones and MLH1. *Cytogenetic and Genome Research* **129**: 143–153.

Chelysheva L, Vezon D, Chambon A, Gendrot G, Pereira L, Lemhemdi A, Vrielynck N, Le Guin S, Novatchkova M, Grelon M. 2012. The Arabidopsis HEI10 is a new ZMM protein related to Zip3. *PLoS Genetics* **8**: e1002799.

Cifuentes M, Rivard M, Pereira L, Chelysheva L, Mercier R. 2013. Haploid meiosis in Arabidopsis: double-strand breaks are formed and repaired but without synapsis and crossovers. *PLoS ONE* **8**: e72431.

Cloud V, Chan Y-L, Grubb J, Budke B, Bishop DK. 2012. Rad51 is an accessory factor for Dmc1-mediated joint molecule formation during meiosis. *Science* **337**: 1222–1225.

Couteau F, Belzile F, Horlow C, Grandjean O, Vezon D, Doutriaux MP. 1999. Random chromosome segregation without meiotic arrest in both male and female meiocytes of a dmc1 mutant of Arabidopsis. *Plant Cell* **11**: 1623–1634.

Crismani W, Girard C, Froger N, Pradillo M, Santos JL, Chelysheva L, Copenhaver GP, Horlow C, Mercier R. 2012. FANCM limits meiotic crossovers. *Science* **336**: 1588–1590.

Crismani W, Portemer V, Froger N, Chelysheva L, Horlow C, Vrielynck N, Mercier R. 2013. MCM8 is required for a pathway of meiotic double-strand break repair independent of DMC1 in *Arabidopsis thaliana*. *PLoS Genetics* **9**: e1003165.

Cromer L, Jolivet S, Horlow C, Chelysheva L, Heyman J, De Jaeger G, Koncz C, De Veylder L, Mercier R. 2013. Centromeric cohesion is protected twice at meiosis, by SHUGOSHINs at anaphase I and by PATRONUS at interkinesis. *Current Biology* **23**: 2090–2099.

Da Ines O, Bazile J, Gallego ME, White CI. 2022. DMC1 attenuates RAD51-mediated recombination in Arabidopsis. *PLoS Genetics* **18**: e1010322.

Da Ines O, Degroote F, Amiard S, Goubely C, Gallego ME, White CI. 2013a. Effects of XRCC2 and RAD51B mutations on somatic and meiotic recombination in *Arabidopsis thaliana*. *The Plant Journal* **74**: 959–970.

Da Ines O, Degroote F, Goubely C, Amiard S, Gallego ME, White CI. 2013b. Meiotic recombination in Arabidopsis is catalysed by DMC1, with RAD51 playing a supporting role. *PLoS Genetics* **9**: e1003787.

Enguita-Marruedo A, Martín-Ruiz M, García E, Gil-Fernández A, Parra MT, Viera A, Rufas JS, Page J. 2019. Transition from a meiotic to a somatic-like

DNA damage response during the pachytene stage in mouse meiosis. *PLoS Genetics* **15**: e1007439.

Farahani-Tafreshi Y, Wei C, Gan P, Daradur J, Riggs CD, Hasenkampf CA. 2022. The Arabidopsis HOP2 gene has a role in preventing illegitimate connections between nonhomologous chromosome regions. *Chromosome Research* **30**: 59–75.

Ferdous M, Higgins JD, Osman K, Lambing C, Roitinger E, Mechtler K, Armstrong SJ, Perry R, Pradillo M, Cuñado N *et al.* 2012. Inter-homolog crossing-over and synapsis in Arabidopsis meiosis are dependent on the chromosome axis protein AtASY3. *PLoS Genetics* **8**: e1002507.

Fernandes JB, Duhamel M, Seguéla-Arnaud M, Froger N, Girard C, Choinard S, Solier V, De Winne N, De Jaeger G, Gevaert K *et al.* 2018a. FIGL1 and its novel partner FLIP form a conserved complex that regulates homologous recombination. *PLoS Genetics* **14**: e1007317.

Fernandes JB, Séguéla-Arnaud M, Larchevêque C, Lloyd AH, Mercier R. 2018b. Unleashing meiotic crossovers in hybrid plants. *Proceedings of the National Academy of Sciences, USA* **115**: 2431–2436.

Fu R, Wang C, Shen H, Zhang J, Higgins JD, Liang W. 2020. Rice OsBRCA2 is required for DNA double-strand break repair in meiotic cells. *Frontiers in Plant Science* **11**: 600820.

Girard C, Chelysheva L, Choinard S, Froger N, Macaisne N, Lehmemdi A, Mazel J, Crismani W, Mercier R. 2015. AAA-ATPase FIDGETIN-LIKE 1 and helicase FANCM antagonize meiotic crossovers by distinct mechanisms. *PLoS Genetics* **11**: e1005369.

Girard C, Crismani W, Froger N, Mazel J, Lemhemdi A, Horlow C, Mercier R. 2014. FANCM-associated proteins MHF1 and MHF2, but not the other Fanconi anemia factors, limit meiotic crossovers. *Nucleic Acids Research* **42**: 9087–9095.

Greenhough LA, Liang C-C, Belan O, Kunzelmann S, Maslen S, Rodrigo-Brenni MC, Anand R, Skehel M, Boulton SJ, West SC. 2023. Structure and function of the RAD51B–RAD51C–RAD51D–XRCC2 tumour suppressor. *Nature* **619**: 650–657.

Hayashi M, Chin GM, Villeneuve AM. 2007. *C. elegans* germ cells switch between distinct modes of double-strand break repair during meiotic prophase progression. *PLoS Genetics* **3**: e191.

Hernandez Sanchez-Rebato M, Bouatta AM, Gallego ME, White CI, Da Ines O. 2021. RAD54 is essential for RAD51-mediated repair of meiotic DSB in Arabidopsis. *PLoS Genetics* **17**: e1008919.

Higgins JD, Sanchez-Moran E, Armstrong SJ, Jones GH, Franklin FCH. 2005. The Arabidopsis synaptonemal complex protein ZYP1 is required for chromosome synapsis and normal fidelity of crossing over. *Genes & Development* **19**: 2488–2500.

Humphryes N, Hochwagen A. 2014. A non-sister act: recombination template choice during meiosis. *Experimental Cell Research* **329**: 53–60.

Hunter N. 2015. Meiotic recombination: the essence of heredity. *Cold Spring Harbor Perspectives in Biology* **7**: a016618.

Hurel A, Phillips D, Vrielynck N, Mézard C, Grelon M, Christophorou N. 2018. A cytological approach to studying meiotic recombination and chromosome dynamics in *Arabidopsis thaliana* male meiocytes in three dimensions. *The Plant Journal* **95**: 385–396.

Ito M, Furukohri A, Matsuzaki K, Fujita Y, Toyoda A, Shinohara A. 2023. FIGNL1 AAA+ ATPase remodels RAD51 and DMC1 filaments in pre-meiotic DNA replication and meiotic recombination. *Nature Communications* **14**: 6857.

Joshi N, Brown MS, Bishop DK, Börner GV. 2015. Gradual implementation of the meiotic recombination program via checkpoint pathways controlled by global DSB levels. *Molecular Cell* **57**: 797–811.

Kerzendorfer C, Vignard J, Pedrosa-Harand A, Siwiec T, Akimcheva S, Jolivet S, Sablowski R, Armstrong S, Schweizer D, Mercier R *et al.* 2006. The *Arabidopsis thaliana MND1* homologue plays a key role in meiotic homologous pairing, synapsis and recombination. *Journal of Cell Science* **119**: 2486–2496.

Kim KP, Weiner BM, Zhang L, Jordan A, Dekker J, Kleckner N. 2010. Sister cohesion and structural axis components mediate homolog bias of meiotic recombination. *Cell* **143**: 924–937.

Kumar R, Duhamel M, Coutant E, Ben-Nahia E, Mercier R. 2019. Antagonism between BRCA2 and FIGL1 regulates homologous recombination. *Nucleic Acids Research* **47**: 5170–5180.

Kurzbauer M-T, Uanschou C, Chen D, Schlögelhofer P. 2012. The recombinases DMC1 and RAD51 are functionally and spatially separated during meiosis in *Arabidopsis*. *Plant Cell* **24**: 2058–2070.

Lambing C, Kuo PC, Tock AJ, Topp SD, Henderson IR. 2020. ASY1 acts as a dosage-dependent antagonist of telomere-led recombination and mediates crossover interference in Arabidopsis. *Proceedings of the National Academy of Sciences, USA* **117**: 13647–13658.

Lao JP, Cloud V, Huang C-C, Grubb J, Thacker D, Lee C-Y, Dresser ME, Hunter N, Bishop DK. 2013. Meiotic crossover control by concerted action of Rad51-Dmc1 in homolog template bias and robust homeostatic regulation. *PLoS Genetics* **9**: e1003978.

Li W, Chen C, Markmann-Mulisch U, Timofejeva L, Schmelzer E, Ma H, Reiss B. 2004. The Arabidopsis AtRAD51 gene is dispensable for vegetative development but required for meiosis. *Proceedings of the National Academy of Sciences, USA* **101**: 10596–10601.

Li X, Zhang J, Huang J, Xu J, Chen Z, Copenhaver GP, Wang Y. 2021. Regulation of interference-sensitive crossover distribution ensures crossover assurance in *Arabidopsis*. *Proceedings of the National Academy of Sciences, USA* **118**: e2107543118.

Liu J, Renault L, Veaute X, Fabre F, Stahlberg H, Heyer W-D. 2011. Rad51 paralogues Rad55-Rad57 balance the antirecombinase Srs2 in Rad51 filament formation. *Nature* **479**: 245–248.

Lloyd A. 2023. Crossover patterning in plants. *Plant Reproduction* **36**: 55–72.

Matsuzaki K, Kondo S, Ishikawa T, Shinohara A. 2019. Human RAD51 paralogue SWSAP1 fosters RAD51 filament by regulating the anti-recombinase FIGNL1 AAA+ ATPase. *Nature Communications* **10**: 1407.

Mercier R, Mézard C, Jenczewski E, Macaisne N, Grelon M. 2015. The molecular biology of meiosis in plants. *Annual Review of Plant Biology* **66**: 297–327.

Morgan C, Nayak A, Hosoya N, Smith GR, Lambing C. 2023. Meiotic chromosome organization and its role in recombination and cancer. *Current Topics in Developmental Biology* **151**: 91–126.

Mu N, Li Y, Li S, Shi W, Shen Y, Yang H, Zhang F, Tang D, Du G, You A *et al.* 2023. MUS81 is required for atypical recombination intermediate resolution but not crossover designation in rice. *New Phytologist* **237**: 2422–2434.

Niu H, Wan L, Busygina V, Kwon Y, Allen JA, Li X, Kunz RC, Kubota K, Wang B, Sung P *et al.* 2009. Regulation of meiotic recombination via Mek1-mediated Rad54 phosphorylation. *Molecular Cell* **36**: 393–404.

Osakabe K, Yoshioka T, Ichikawa H, Toki S. 2002. Molecular cloning and characterization of RAD51-like genes from *Arabidopsis thaliana*. *Plant Molecular Biology* **50**: 71–81.

Osman K, Desjardins SD, Simmonds J, Burridge AJ, Kanyuka K, Henderson IR, Edwards KJ, Uauy C, Franklin FCH, Higgins JD *et al.* 2024. FIGL1 prevents aberrant chromosome associations and fragmentation and limits crossovers in polyploid wheat meiosis. *New Phytologist* **244**: 528–541.

Panoli AP, Ravi M, Sebastian J, Nishal B, Reddy TV, Marimuthu MPA, Subbiah V, Vijaybhaskar V, Siddiqi I. 2006. AtMND1 is required for homologous pairing during meiosis in Arabidopsis. *BMC Molecular Biology* **7**: 24.

Petukhova GV, Pezza RJ, Vanevski F, Ploquin M, Masson J-Y, Camerini-Otero RD. 2005. The Hop2 and Mnd1 proteins act in concert with Rad51 and Dmc1 in meiotic recombination. *Nature Structural & Molecular Biology* **12**: 449–453.

Ravi M, Chan SWL. 2010. Haploid plants produced by centromere-mediated genome elimination. *Nature* **464**: 615–618.

Rawal Y, Jia L, Meir A, Zhou S, Kaur H, Ruben EA, Kwon Y, Bernstein KA, Jasin M, Taylor AB *et al.* 2023. Structural insights into BCDX2 complex function in homologous recombination. *Nature* **619**: 640–649.

Ross KJ, Fransz P, Jones GH. 1996. A light microscopic atlas of meiosis in *Arabidopsis thaliana*. *Chromosome Research* **4**: 507–516.

Sanchez-Moran E, Santos J-L, Jones GH, Franklin FCH. 2007. ASY1 mediates AtDMC1-dependent interhomolog recombination during meiosis in Arabidopsis. *Genes & Development* **21**: 2220–2233.

Schwacha A, Kleckner N. 1994. Identification of joint molecules that form frequently between homologs but rarely between sister chromatids during yeast meiosis. *Cell* **76**: 51–63.

Schwacha A, Kleckner N. 1997. Interhomolog bias during meiotic recombination: meiotic functions promote a highly differentiated interhomolog-only pathway. *Cell* **90**: 1123–1135.

Seeliger K, Dukowic-Schulze S, Wurz-Wildersinn R, Pacher M, Puchta H. 2012. BRCA2 is a mediator of RAD51- and DMC1-facilitated homologous recombination in *Arabidopsis thaliana*. *New Phytologist* **193**: 364–375.

Séguéla-Arnaud M, Choinard S, Larchevêque C, Girard C, Froger N, Crismani W, Mercier R. 2017. RMI1 and TOP3α limit meiotic CO formation through their C-terminal domains. *Nucleic Acids Research* **45**: 1860–1871.

Séguéla-Arnaud M, Crismani W, Larchevêque C, Mazel J, Froger N, Choinard S, Lemhemdi A, Macaisne N, Van Leene J, Gevaert K *et al.* 2015. Multiple mechanisms limit meiotic crossovers: TOP3α and two BLM homologs antagonize crossovers in parallel to FANCM. *Proceedings of the National Academy of Sciences, USA* **112**: 4713–4718.

Sheridan SD, Yu X, Roth R, Heuser JE, Sehorn MG, Sung P, Egelman EH, Bishop DK. 2008. A comparative analysis of Dmc1 and Rad51 nucleoprotein filaments. *Nucleic Acids Research* **36**: 4057–4066.

Slotman JA, Paul MW, Carofiglio F, De Gruiter HM, Vergroesen T, Koornneef L, Van Cappellen WA, Houtsmuller AB, Baarends WM. 2020. Super-resolution imaging of RAD51 and DMC1 in DNA repair foci reveals dynamic distribution patterns in meiotic prophase. *PLoS Genetics* **16**: e1008595.

Stronghill P, Pathan N, Ha H, Supijono E, Hasenkampf C. 2010. Ahp2 (Hop2) function in *Arabidopsis thaliana* (Ler) is required for stabilization of close alignment and synaptonemal complex formation except for the two short arms that contain nucleolus organizer regions. *Chromosoma* **119**: 443–458.

Thacker J. 2005. The RAD51 gene family, genetic instability and cancer. *Cancer Letters* **219**: 125–135.

Toraason E, Horacek A, Clark C, Glover ML, Adler VL, Premkumar T, Salagean A, Cole F, Libuda DE. 2021. Meiotic DNA break repair can utilize homolog-independent chromatid templates in *C. elegans*. *Current Biology* **31**: 1508–1514.

Tsubouchi H, Roeder GS. 2006. Budding yeast Hed1 down-regulates the mitotic recombination machinery when meiotic recombination is impaired. *Genes & Development* **20**: 1766–1775.

Uanschou C, Ronceret A, Von Harder M, De Muyt A, Vezon D, Pereira L, Chelysheva L, Kobayashi W, Kurumizaka H, Schlögelhofer P *et al.* 2014. Sufficient amounts of functional HOP2/MND1 complex promote interhomolog DNA repair but are dispensable for intersister DNA repair during meiosis in *Arabidopsis*. *Plant Cell* **25**: 4924–4940.

Vignard J, Siwiec T, Chelysheva L, Vrielynck N, Gonord F, Armstrong SJ, Schlögelhofer P, Mercier R. 2007. The interplay of RecA-related proteins and the MND1-HOP2 complex during meiosis in *Arabidopsis thaliana*. *PLoS Genetics* **3**: 1894–1906.

Vrielynck N, Peuch M, Durand S, Lian Q, Chambon A, Hurel A, Guérin J, Guérois R, Mercier R, Grelon M *et al.* 2023. SCEP1 and SCEP2 are two new components of the synaptonemal complex central element. *Nature Plants* **9**: 2016–2030.

Wang H, Hu Q, Tang D, Liu X, Du G, Shen Y, Li Y, Cheng Z. 2016. OsDMC1 is not required for homologous pairing in rice meiosis. *Plant Physiology* **171**: 230–241.

Wang S, Zickler D, Kleckner N, Zhang L. 2015. Meiotic crossover patterns: obligatory crossover, interference and homeostasis in a single process. *Cell Cycle* **14**: 305–314.

Wang Y, Copenhaver GP. 2018. Meiotic recombination: mixing it up in plants. *Annual Review of Plant Biology* **69**: 577–609.

Wang Y, Xiao R, Wang H, Cheng Z, Li W, Zhu G, Wang Y, Ma H. 2014. The Arabidopsis RAD51 paralogs RAD51B, RAD51D and XRCC2 play partially redundant roles in somatic DNA repair and gene regulation. *New Phytologist* **201**: 292–304.

Yang S, Zhang C, Cao Y, Du G, Tang D, Li Y, Shen Y, Yu H, Cheng Z. 2022. FIGNL1 inhibits non-homologous chromosome association and crossover formation. *Frontiers in Plant Science* **13**: 945893.

Yuan J, Chen J. 2013. FIGNL1-containing protein complex is required for efficient homologous recombination repair. *Proceedings of the National Academy of Sciences, USA* **110**: 10640–10645.

Zhang F, Shen Y, Miao C, Cao Y, Shi W, Du G, Tang D, Li Y, Luo Q, Cheng Z. 2020. OsRAD51D promotes homologous pairing and recombination by preventing nonhomologous interactions in rice meiosis. *New Phytologist* **227**: 824–839.

Zhang F, Shi W, Zhou Y, Ma L, Miao Y, Mu N, Ren H, Cheng Z. 2023. RAD51C-RAD51D interplays with MSH5 and regulates crossover maturation in rice meiosis. *New Phytologist* **239**: 1790–1803.

Zhang P, Zhang Y, Sun L, Sinumporn S, Yang Z, Sun B, Xuan D, Li Z, Yu P, Wu W *et al.* 2017. The rice AAA-ATPase OsFIGNL1 is essential for male meiosis. *Frontiers in Plant Science* **8**: 1639.

Zhang Q, Fan J, Xu W, Cao H, Qiu C, Xiong Y, Zhao H, Wang Y, Huang J, Yu C. 2023. The FLIP-FIGNL1 complex regulates the dissociation of RAD51/DMC1 in homologous recombination and replication fork restart. *Nucleic Acids Research* **51**: 8606–8622.

Zhang T, Zhao S, Wang Y, He Y. 2023. FIGL1 coordinates with dosage-sensitive BRCA2 in modulating meiotic recombination in maize. *Journal of Integrative Plant Biology* **65**: 2107–2121.

Ziesel A, Weng Q, Ahuja JS, Bhattacharya A, Dutta R, Cheng E, Börner GV, Lichten M, Hollingsworth NM. 2022. Rad51-mediated interhomolog recombination during budding yeast meiosis is promoted by the meiotic recombination checkpoint and the conserved Pif1 helicase. *PLoS Genetics* **18**: e1010407.

Supporting Information

Additional Supporting Information may be found online in the Supporting Information section at the end of the article.

Dataset S1 SeedCount.

Dataset S2 BivalentCount.

Fig. S1 Functional interaction between *figl1* and *rad51*.

Fig. S2 Interaction models of XRCC2, RAD51B, and FRBD-FIGL1.

Fig. S3 Functional interaction between *figl1* and *dmc1*.

Fig. S4 Analysis of synaptonemal complex assembly.

Please note: Wiley is not responsible for the content or functionality of any Supporting Information supplied by the authors. Any queries (other than missing material) should be directed to the *New Phytologist* Central Office.